MICROSTRUCTURE AND CHEMISTRY EVALUATION OF DIRECT METAL LASER SINTERED
15-5 PH STAINLESS STEEL

by

KEVIN M. COFFY
B.S.M.E. University of Central Florida, 2012

A thesis submitted in partial fulfillment of the requirements
for the degree of Master of Science
in the Department of Materials Science and Engineering
in the College of Engineering and Computer Science
at the University of Central Florida
Orlando, Florida

Summer Term
2014

ABSTRACT

15-5PH stainless steel is an important alloy in the aerospace, chemical, and nuclear industries for its high strength and corrosion resistance at high temperature. Thus, this material is a good candidate for processing development in the direct metal laser sintering (DMLS) branch of additive manufacturing. The chemistry and microstructure of this alloy processed via DMLS was compared to its conventionally cast counterpart through various heat treatments as part of a characterization effort. The investigation utilized optical microscopy, scanning electron microscopy (SEM), transmission electron microscopy (TEM), X-Ray diffractometry (XRD), energy dispersive X-Ray spectroscopy (EDS) and glow discharge atomic emission spectrometry (GDS) techniques. DMLS processed samples contained a layered microstructure in which the prior austenite grain sizes were relatively smaller than the cast and annealed prior austenite grain size. The largest of the quantifiable DMLS prior austenite grains had an ASTM grain size of approximately 11.5-12 (6.7μm to 5.6μm, respectively) and the cast and annealed prior austenite grain size was approximately 7-7.5 (31.8μm to 26.7μm, respectively), giving insight to the elevated mechanical properties of the DMLS processed alloy. During investigation, significant amounts of retained austenite phase were found in the DMLS processed samples and quantified by XRD analysis. Causes of this phase included high nitrogen content, absorbed during nitrogen gas atomization of the DMLS metal powder and from the DMLS build chamber nitrogen atmosphere. Nitrogen content was quantified by GDS for three samples. DMLS powder produced by nitrogen gas atomization had a nitrogen content of 0.11 wt%. A DMLS processed sample contained 0.08 wt% nitrogen, and a conventionally cast and annealed sample contained only 0.019 wt% nitrogen. In iron based alloys, nitrogen is a

significant austenite promoter and reduced the martensite start and finish temperatures, rendering the standard heat treatments for the alloy ineffective in producing full transformation to martensite. Process improvements are proposed along with suggested future research.

ACKNOWLEDGMENTS

TABLE OF CONTENTS

LIST OF FIGURES

LIST OF TABLES

LIST OF ACRONYMS

2α	Diffraction angle of the monochromator crystal
A	Cross sectional area of the incident beam
BCC	Body Centered Cubic
BCT	Body Centered Tetragonal
c	Velocity of light
DMLS	Direct Metal Laser Sintered
e	Charge of an electron
e^{-2M}	Debye-Waller or temperature factor
EDS	Energy Dispersive X-ray Spectroscopy
$/F/^2$	Structure factor times its complex conjugate
FCC	Face Centered Cubic crystal structure
GDS	Glow Discharge Atomic Emission Spectrometry
FIB	Focused Ion Beam
$I_{\alpha'}{}^{hkl}$	Integrated intensity per angular diffraction peak (hkl) in the α'-phase
I_o	Intensity of the incident beam
λ	Wavelength of incident radiation
LP	Lorentz Polarization factor
m	Mass of an electron
μ	Linear absorption coefficient for the steel
$\mu_s{}^2$	Mean square displacement of the atoms from their mean position, in a direction perpendicular to the diffracting plane
p	Multiplicity factor of the (hkl) reflection
r	Radius of the diffractometer
SADP	Selected Area Diffraction Pattern

SEM	Scanning Electron Microscope
TEM	Transmission Electron Microscope
UNS	Unified Numbering System
θ	Bragg angle
v	Volume of the unit cell
$V_{\alpha'}$	Volume fraction of the α'-phase
Vol.%	Volume percent
wt%	Weight percent

CHAPTER 1: INTRODUCTION

The role of direct metal laser sintering (DMLS) has grown exponentially in the past decade. Commercial machines are now available but limited to those able to afford the high costs of developing technology. The process is carving out its niche in the manufacturing arena. The multidisciplinary machine combines principles from materials science, mechanical engineering, and optics to stream line a process which can build parts with even finer precision than most large scale machine shops.

As a method of three-dimensional printing, the DMLS process is an automated manufacturing process using a growing variety of metal alloys for creation of parts. New applications for the process are developing at rapid rates. It is used in many industries including patient customized dental implants, customized replacement prosthetic joints, and complex parts for gas turbine engines and the defense industry. This increasingly useful technique is consistently proving quicker turnarounds on part production and greater freedom of design geometry all the while lowering costs compared with traditional manufacturing techniques.

However, while this manufacturing method does seem promising, much more research and characterization is necessary to qualify and expand the process as an industry standard using a variety of new materials. The modern process employed in DMLS manufacturing is quite complex. The complexities arise in the variables and fine tuning to produce higher quality part resolution and enhanced material properties.

Ideally, DMLS parts will be end-use parts or tooling parts ready for use directly out of the machine. However, this is only the case for heavily studied processing for certain materials, and in most cases DMLS parts generally must undergo a heat treatment and

surface finishing. Surface roughness can be an issue for certain applications, and will need post machining or processing to obtain the desired surface characteristics.

The strengths and weaknesses of DMLS in the manufacturing industry remain under investigation. Some advantages of additive manufacturing over conventional or subtractive manufacturing are a more automated process, shorter turnaround times, low waste, tight tolerances, lower cost for small quantities, high end material properties, greater ability to create complex geometries and simple customized changes to parts.

The automated process allows for the little manpower of a few trained machine operators to set up the DMLS machine, upload part data and allow it to run. Once the machine is running, the crew is free to prepare the CAD file for the next part. A large advantage to this process is that the machine is capable of creating parts during nonstandard business hours without supervision. This greatly improves productivity since parts are being created after employees have clocked out. When they return the next day, the parts can be removed from the machine and then next set of parts can be set up to run. The speed of the machine and the ability for it to run during non-working hours greatly contributes to the fast turnaround. When compared to traditional machining which requires a well thought out series of subtractive processes with constant supervision and frequent input from operators, additive manufacturing clearly has an advantage. When comparing the waste of additive to traditional manufacturing, DMLS only uses the powder required to build the part and the rest may be reused. This is a very economical process compared to subtractive methods, which by their name implies that scraps are generated.

These advantages of additive manufacturing contribute to lower overall cost for producing the same parts as created by traditional manufacturing techniques. The processes use less stock material, time and energy than traditional manufacturing

procedures, thus lowering cost and reducing waste. Beyond lower cost, the quality of the materials used must be considered. In general, the mechanical properties of the materials produced out of the DMLS machine tend to be on the higher end of the traditional mechanical properties spectrum. Even after applying a stress relieving heat treatment, most properties remain in that upper level range when compared to their conventionally cast counterparts (ASTM International, 2013). These properties can be compared in the material specification sheets provided by a steel manufacturer and EOS (AK Steel Corporation, 2007) (EOS GmbH - Electro Optical Systems, 2012). Key contributors to these elevated properties of the DMLS processed 15-5PH are discussed in chapter 5 of this thesis.

The process of building layer by layer in additive manufacturing allows for more complex geometries to be created. This allows for such applications of interconnected parts, metal meshes, and a reduced need for welding which can greatly strengthen an overall structure.

However, there are recognized disadvantages to the additive manufacturing process. Defects, as with all materials and manufacturing processes, are a large issue. Additive manufacturing materials come in a powder form before they are sintered and therefore are inherently exposed to oxygen and humidity from the atmosphere. This may contribute to oxidation and corrosion on the surfaces of the powders prior to sintering and may be carried over into the post DMLS processed material. These material defects and impurities may contribute to the embrittlement and lattice strain of the laser sintered material. Besides these surface oxidation and corrosion issues, the powder is produced via gas atomization in a nitrogen atmosphere, which may alter the chemistry of the alloy during the process. Internal stresses are also an issue when laser sintering layer by layer. A quench induced residual stress is the result of this process but can be minimized with a

stress relieving heat treatment at the expense of reducing some of the mechanical properties closer to the range of typical wrought properties. Directly out of the machine the parts have a somewhat rough surface which may need to be cleaned and polished if a finer surface roughness is desired. Another disadvantage of additive manufacturing is the lack of full characterization over a wide range of materials. This is currently underway and warrants a need for much future research to be conducted.

The specific alloy of study for the purpose of this thesis is 15-5 PH (UNS S15500). This alloy is used in the aerospace, petrochemical and nuclear industries, among others, for high strength and corrosion resistance at high temperatures.

The potentials for this alloy as processed by DMLS are increased geometric freedom of design, lower cost customized production with a quick turnaround time from order to finished part, and a reduction in waste when compared to a traditional manufacturing process. Such design freedom would allow for advantages such as weight reduction of aerospace parts, customized single piece heat exchangers with curved cooling channels, or skipped production steps such as integrated fittings for hardware or hollow sections. The reduction in waste is achieved by only using the amount of material required for the part. The remaining unsintered powder can be collected and reused.

The objective of this study is to investigate the microstructure and composition of laser sintered 15-5PH stainless steel through a variety of characterization methods to provide insight for processing improvements.

CHAPTER 2: LITERATURE REVIEW

2.1 15-5 PH Stainless Steel

The 15-5 PH stainless steel is a complex alloy designed to produce a range of

mechanical properties with varying heat treatments. The alloy is also known by its Unified

Numbering System (UNS) designation of S15500. Any variation in the mechanical

properties of the alloy could be traced to a nonconformance in composition, a variation in

heat treatment, or manufacturing process.

The manufacturer of this alloy is Electro Optical Systems based out of Munich,

Germany. This company is a leader is the commercialization of DMLS among other types of

additive manufacturing. EOS is the producer of 15-5PH steel powder and the EOS M270

DMLS machine in this study.

The composition of this alloy is given in **Table 1**:

Table 1: Elemental Composition of 15-5PH (EOS GmbH - Electro Optical Systems, 2012)

Element	Weight Percent (wt%)
Iron, Fe	Balance
Chromium, Cr	14 - 15.5
Nickel, Ni	3.5 – 5.5
Copper, Cu	2.5 – 4.5
Manganese, Mn	Max. 1
Silicon, Si	Max 1
Molybdenum, Mo	Max. 0.5
Niobium, Nb	0.15 – 0.45
Carbon, C	Max. 0.07

Each element is carefully balanced to play a specific role in the mechanical and chemical resistance properties of the alloy. Starting with iron, the advantages of iron based alloys include low cost, high strength, and, with additions of other alloying elements, this base metal can produce a large range of chemical and physical properties for a variety of applications. This makes it one most common elements used in engineering applications. Chromium is used to increase corrosion resistance by creating an impermeable Cr_2O_3 scale on the alloy to reduce further corrosion. It also contributes to the stabilization of the martensite body centered cubic (BCC) phase. Nickel is also used to increase corrosion resistance and toughness of the alloy. It is an austenite face centered cubic (FCC) phase stabilizing element. Copper is an element added for its precipitation hardening effects. During the final precipitation hardening heat treatment, a copper-rich ε-phase nucleates and grows until a designed particle size of 4nm to 45nm is reached based on the selected

precipitation hardening heat treatment (ASHOK KUMAR, 2013). The copper rich precipitates with nucleate and form a spherical shape with a 9R crystal structure and grow with higher temperature heat treatments to become elliptical in shape and have an FCC crystal structure (Bajguirani, 2002). These particle sizes are effective in impeding dislocation movement and provide a semi-coherent interface, therefore hardening the alloy. Other minor elements (<2 wt%) in 15-5 PH can have a large effect. Manganese is kept higher than the expected sulfur content and acts as a sulfur getter. Manganese sulfides form evenly throughout the grains instead of the detrimental iron sulfides at grain boundaries. Manganese is limited because is it an austenite stabilizer. Excess quantities have a similar effect as nickel. Silicon is also useful in limited quantities. Small amounts will increase corrosion resistance but larger amounts can cause unwanted brittle phases to form. It is also a martensite/ferrite phase promoting element. Molybdenum is also a martensite/ferrite phase promoting element and, in small quantities, can increase corrosion resistance when paired with chromium. In controlled amounts, niobium will preferentially getter carbon to form carbides that are less harmful to the alloy than other undesired carbides that would otherwise form. They will form preferentially in the martensite lath and grow to a size of approximately 35nm to 45nm (Bajguirani, 2002). It is also a martensite/ferrite phase promoter. Carbon is limited because in excess it preferentially precipitates carbides in grain boundaries and it promotes austenite phase formation. Another element of note, not included in the composition above, is nitrogen. It is a strong austenite phase promoter and can increase hardness at the expense of ductility (ASM International, 2005).

2.2 Processing

Conventional production of 15-5 PH stainless steel begins with casting and then extruding or rolling the alloy. The alloy is subsequently annealed to refine the grain shapes and sizes and is delivered in this condition, referred to as condition A, to the customer. The customer will then machine the alloy into the final manufactured shape and apply a precipitation hardening heat treatment tailored to obtain the desired material properties for the application.

2.2.1 Powder Manufacture

The DMLS and conventional material production process both begin with a chemistry balanced melt. The melting temperature for15-5 PH stainless steel is 1400 – 1440°C within compositional tolerances (ASM International, 2005). For the DMLS material, the melt is gas atomized by forcing the melt into a chamber of nitrogen gas circulating at supersonic speeds. The melt disperses and forms finely dispersed microscopic droplets that solidify and quench. The powder is filtered from the chamber and collected at an outlet. This process is schematically illustrated in **Figure 1**. The powder is filtered to produce a Gaussian distribution of particles and is marketed as the product for use in the DMLS machines produced by EOS GmbH.
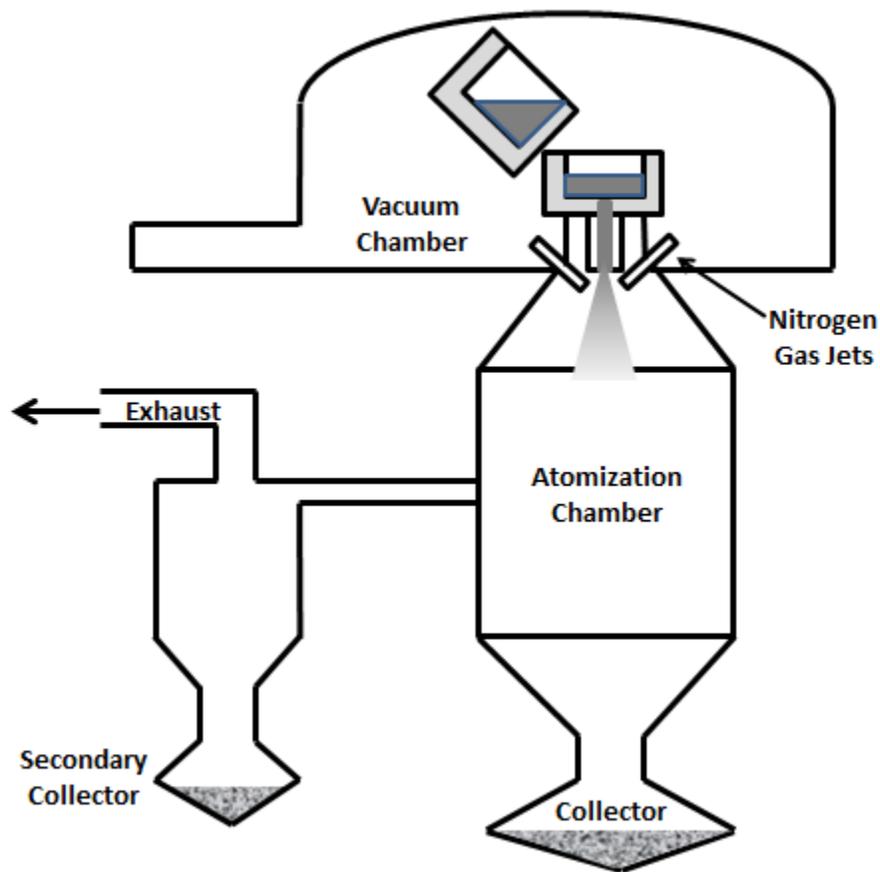
Figure 1: Gas Atomization Process

2.2.2 Direct Metal Laser Sintering Process

The DMLS operator receives the powder in a hermetically sealed container but once opened, the powder is exposed to the ambient conditions of the facility in which it is processed. The operator pours the powder into the powder delivery reservoir while wearing nitrile or latex gloves, safety glasses and a respirator. The machine can operate with either a nitrogen or argon atmosphere. In the case of producing parts from 15-5 PH, the manufacturer recommended that a nitrogen atmosphere be used. Any powder remaining after a production run can be reused in subsequent runs. This re-used type of powder is referred to as "recycled powder". Powder that has not been placed on the build

stage during a run is considered to be "fresh powder". As-built parts, directly out of the

DMLS machine, are considered by the manufacturer to be in a similar condition to the

supplied annealed condition (condition A) of the conventionally produced material.

The process begins by applying a thin layer of metal powder onto a substrate with a

roller. A computer aided design (CAD) file is downloaded and converted to a standard

stereolithography (.stl) file format by the software on the machine. According to the

geometry loaded into the DMLS machine, the laser will trace over a cross-section and sinter

the powder into a solid layer using process parameters either specified by the operator or

recommended by the manufacturer. This process is schematically described in **Figure 2**.

The unsintered powder will remain on the substrate and act as a support for the next layer.

This process is repeated by rolling another layer of metal powder over the previous layer

and tracing out the next cross-section. Layer by layer, the geometry is built in the vertical

(z-axis) direction until the final part is formed. The part will cool in the machine with a

controlled atmosphere and can then be removed from the machine. The remaining

unsintered metal powder is collected and can be reused for another build cycle. Because

the powder can be reused, the process creates very little waste in comparison to traditional

subtractive manufacturing.
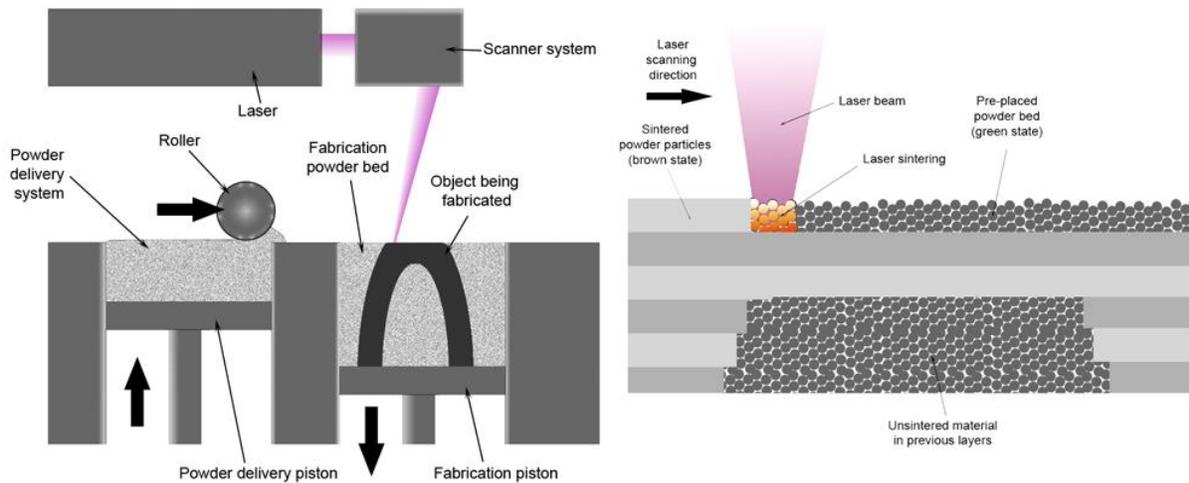
Figure 2: Direct Metal Laser Sintering Process (Materialgeeza, 2008)

2.2.3 Heat Treatment

Various heat treatments can be applied to the material at this stage from either production method. These heat treatments are selected based on the desired mechanical properties for the application of the part. The key difference between the heat treatments of the conventionally produced material and the DMLS processed material is that the latter is recommended by the manufacturer to forgo the solution anneal outlined in *AMS 2759/3E Heat Treatment Precipitation-Hardening Corrosion-Resistant and Maraging Steel Parts* (SAE International, 2008). The reasoning behind this is that the manufacturer claims that the material is in the solution annealed state when the DMLS building process is complete. For both processing routes, a subsequent heat treatment below the reaustenization temperature is required for stress relief and precipitation hardening.

2.2.4 Processing Conditions

Precautions need to be taken in all steps of production, from balancing the chemistry of the melt through final heat treatment. High carbon levels in the melt are a common issue and are carefully controlled with the carbon limited to 0.07 wt%. Atmosphere control is another important aspect of processing. Gasses and impurities may react with the alloy in different settings producing unintended results.

The manufacturer of the alloy powder of study recommends processing the powder via DMLS in a nitrogen atmosphere to reduce oxidation. However, it should be noted that once the hermetically sealed powder container is opened, it is exposed to the atmosphere of the room, including oxygen and humidity at room temperature, until it is processed by the machine. In addition, some powder that is moved to the build stage of the machine during sintering but not sintered into a production piece can be collected and recycled into the machine again. This "recycled" powder has been exposed to a variable amount of heat from the heat accumulation in the build chamber depending on its proximity to a sintered surface.

2.3 Phase Transformation

By design, 15-5PH has a martensitic structure upon cooling from the melt (AK Steel Corporation, 2007) (ASM International, 1992). This martensitic structure is transformed from an austenitic structure with rapid cooling when a martensitic phase transformation temperature is reached.

2.3.1 Crystal Structure

Upon heating of the alloy, the atoms form an FCC structure referred to as austenite and designated as the γ-phase. This phase is of disordered structure, meaning that the alloy atoms are not in a strict order. The alloying elements mix into the lattice with iron substitutionally and interstitially. The Hume-Rothery rules apply in this situation by which the substitutional atoms are similar in size, electronegativity, and valency. The smaller atoms, such as carbon or nitrogen, are either included in the composition or are impurities gathered in processing gather in the interstitial sites in the lattice. In the austenite phase these smaller atoms diffuse to the center of each FCC cell at the (½, ½, ½) position (R. E. Smallman, 2007, pp. 80-81). The local stresses and strains caused by these substitutional and interstitial atoms raises the internal energy of the lattice and thus the free energy barrier for dislocation movement (Joel I. Gersten, 2001) (R. E. Smallman, 2007).

Upon cooling the alloy will reach a phase transformation temperature known as the martensite starting temperature, M_s. This temperature, along with the martensite finish temperature, M_f, will vary with types and amounts of alloying elements. Martensite, in this alloy, is a phase with a BCC structure that is supersaturated with alloying elements. Martensite is commonly found in literature in ferrous alloys with a body centered tetragonal (BCT) lattice with significant carbon content. This is because there is sufficient carbon content to gather in the octahedral interstitial spaces in the (002) plane, forcing a distortion in the z-direction of the lattice and increasing the c/a ratio. 15-5 PH has very low carbon content which will cause a slight extension, at most, on the affected lattice structure but the random orientation averages out to a statistically cubic structure (R. E. Smallman, 2007). The phase transformation from austenite to martensite is a diffusionless process that reorders atoms from an FCC lattice to a BCC lattice. This process includes a slight

volume increase along with a shape change which causes internal stresses (Rober W. Balluffi, 2005). These stresses are reduced with a tempering heat treatment.

2.3.2 Microstructure

The microstructure of 15-5PH is a fully lath martensitic structure with evenly dispersed copper rich precipitates grown during a precipitation hardening heat treatment to increase strength and hardness. These precipitates have been shown to be approximately 5nm in diameter (Bajguirani, 2002). The lath martensitic microstructure is similar to other low carbon steel alloys. The microstructure cannot be observed under an optical microscope until the specimen has been polished and etched. Certain etchants can reveal the prior austenite grain boundaries. The size and shape of the prior austenite grain boundaries show the cooling and deformation history of the sample.

The alloying elements each have an effect on the phase stabilization of 15-5PH. These effects have been studied and summarized in a diagram known as a Schaeffler diagram which accounts for the composition of each austenite and martensite phase stabilizing element with weighted values. Total equivalent austenite stabilizing composition is described as equivalent nickel, Ni_{eq}, and is given a calculated value along the y-axis. The total equivalent martensite stabilizing composition is described as equivalent chromium, Cr_{eq}, and is given a calculated value along the x-axis. The point of intersection is used to predict the phase constituents of the alloy as shown in **Figure 3**. The sections are labeled "A" for austenite, "M" for martensite and "F" for ferrite.
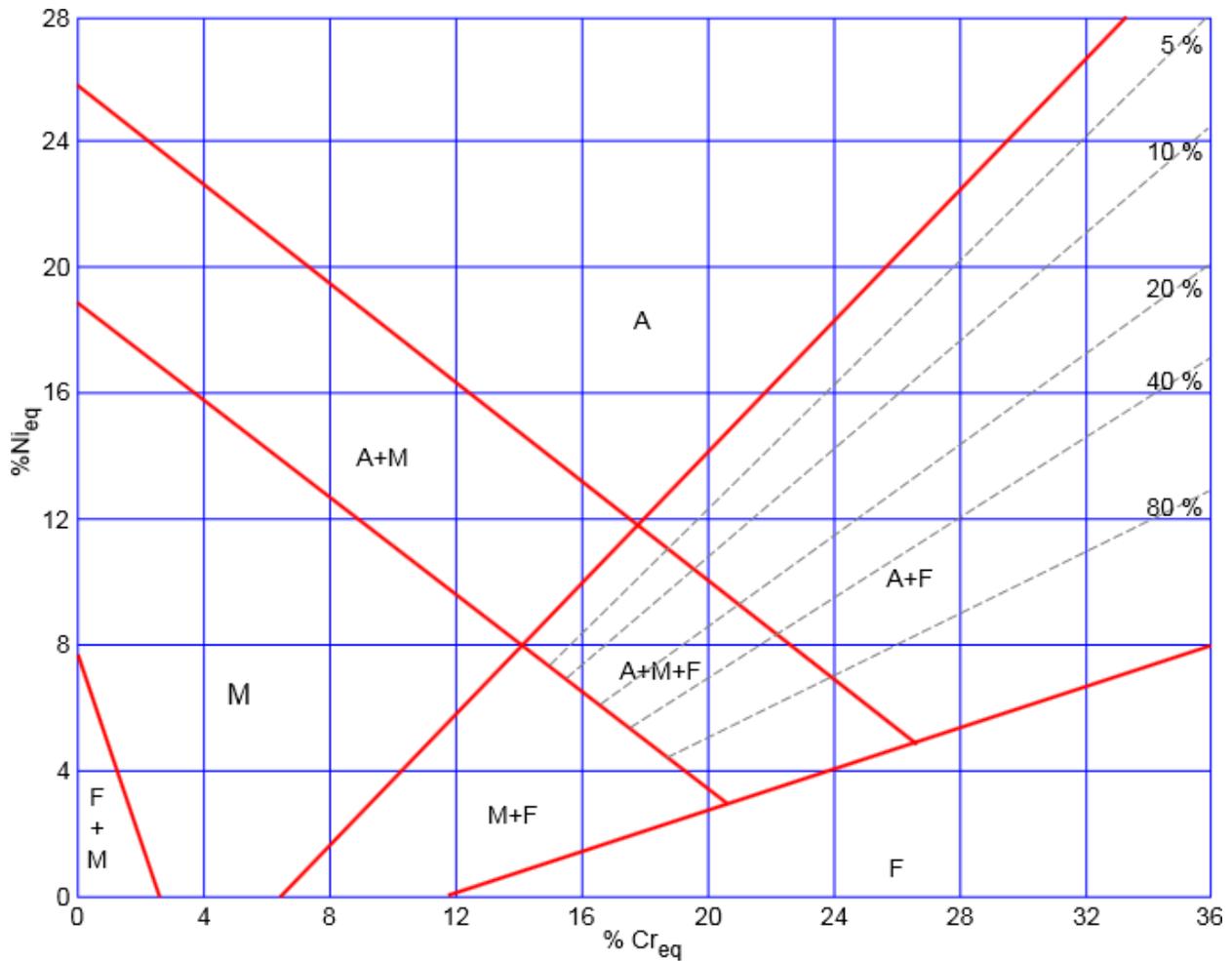
Figure 3: Schaeffler Diagram (Cdang, 2009)

The equations for calculating equivalent nickel and chromium were specified by Schaeffler but did not account for the effect of nitrogen content in the alloy (Schaeffler, 1949). It was not until 1973 that C. J. Long and W. T. Delong added the effect of nitrogen content into the equations given below (C. J. Long, 1973). All percent values are in wt%:

$$Ni_{eq} = \%Ni + 30 \times \%C + 30 \times \%N + 0.5 \times \%Mn \tag{1}$$

$$Cr_{eq} = \%Cr + \%Mo + 1.5 \times \%Si + 0.5 \times \%Nb \tag{2}$$

In the DMLS processed samples, orientation of the processing is observed. The layering of the melt creates a residual outline of the melt pool approximately equal to the layer thickness. In addition, within the melt pool outline, a grain size gradient can be observed correlating with the rapid cooling rates achieved during solidification. In addition to the layering effect, it has been reported that a chemical segregation occurs in the microstructure upon precipitation heat treatment. This effect was described as microstructural banding by chemical segregation by Kumar et al. (ASHOK KUMAR, 2013).

CHAPTER 3: EXPERIMENTAL DETAILS

The experimental path of this investigation began with the intent to utilize standard characterization methods to characterize the microstructure of the DMLS processed alloy against the conventionally processed alloy. During the investigation, unexpected features were revealed which shifted the focus of the investigation and thus the experimental path as outlined in this chapter.

3.1 Materials

Samples of laser sintered 15-5PH and conventionally cast and extruded bar 15-5PH alloy, as a comparable baseline, were acquired. Both materials were verified through elemental analysis by energy dispersive X-ray spectroscopy (EDS) to be within the specified acceptable range for the alloy (EOS GmbH - Electro Optical Systems, 2012). **Table 2** lists the samples evaluated during the study.

Table 2: Samples Used in Experiment

DMLS Processed	Conventionally Processed
Gas atomized powder	N/A
As-Sintered (No Heat Treatment)	Annealed (Condition A)
LH900 Heat Treatment	H900 Heat Treatment
LH1025 Heat Treatment	H1025 Heat Treatment
LH1150 Heat Treatment	H1150 Heat Treatment

Note: see section 3.2 for detailed description of heat treatment.

The type of laser sintering machine employed to produce the laser sintered samples in this investigation was the EOS M270 manufactured by Electro Optical Systems or EOS

GmbH based out of Munich, Germany. The machine was equipped with an upgrade kit featuring an optional argon atmosphere.

The processing parameters used to produce the parts for this study were recommended by EOS for the use on the 15-5 PH equivalent alloy in the EOS M270 DMLS machine. The laser power determines the energy transfer into the material and must be high enough for full sintering of the layer for good adhesion with the previous layer but not too high as to cause over-sintering. The hatching distance is the distance between laser consecutive laser passes. It causes approximately one quarter of the effective laser diameter to create an overlap distance between laser hatchings for full sintering of the powder. The scan speed is the rate at which the laser raster will pass the laser over the build stage. The beam offset applies to the edges of cross-sections of the part. It is an adjustment of the beam one half of the effective laser diameter away from the edge. The purpose of this is to keep the part dimensions as close as possible to the CAD dimensions without sintering any excess powder (Aulus Roberto Romão Bineli, 2011). The parameters recommend are given in **Table 3** (P.P. Bandyopadhyay, 2013)

Table 3: Manufacturer suggested parameters for 15-5PH on EOS M270.

Parameter	Value
Laser Power	195W
Hatching Distance	0.1mm
Overlap	0.05mm
Scan Speed	800mm/s
Beam Offset	0.060mm

3.2 Heat Treatment

A range of heat treatments were of interest and, thus, included in the scope of this investigation. These heat treatments were applied to both the laser sintered and the conventional alloy. The heat treatments applied to the both materials are designated as H900, H1025 and H1150 and are defined in AMS 2759/3E (SAE International, 2008).The heat treatment specification includes an initial solution heat treatment at 1900°F (1038°C) for 1 hour followed by an aging heat treatment to a corresponding temperature of either 900°F (482°C) for 1 hour, or either 1025°F (552°C) or 1150°F (621°C) for 4 hours depending on the desired mechanical properties. However, the manufacturer of the DMLS machine has claimed that the laser sintered products are similar to the annealing heat treatment out of the DMLS machine and therefore do not need to be put through a separate annealing heat treatment before aging. This modified heat treatment is referred to as LH900, LH1025, and LH1150. The "L" in the name indicates a modified heat treatment without the solution anneal step (EOS GmbH - Electro Optical Systems, 2012). Heat treatments were performed following the procedure specified in *AMS 2759/3E* (SAE International, 2008).

3.3 Optical Microscopic Examination

In preparation for examination under the optical microscope, the samples were finely polished and etched to expose the microstructure. The grinding and polishing process began with 240 grit silicon dioxide paper on an automatic polisher using water as lubrication and progressed through 1200 grit silicon dioxide paper. The samples were given a final polishing using 0.25μm diamond paste on a polishing pad.

Much care was taken during the grinding and polishing process to not over polish or use worn out paper. Paper was changed frequently and pressure forced on the samples was monitored. The reason for the extra care is that martensitic structures can revert back to austenitic structures with deformation and excess heat (ASTM International, 2013).

Etching of the samples was necessary to reveal the microstructure. Vilella's reagent was chosen from the list of etchants in *ASTM E407-07 Standard Practice for Microetching Metals and Alloys* (ASTM International, 2007). This etchant was chosen because it is effective in revealing prior austenitic grain boundaries in heat treated martensitic stainless steels. The composition of the etchant is given as 5mL Hydrochloric acid, 1g picric acid, and 100mL of ethanol or methanol (95%). Proper personal protective equipment was utilized when etching was performed as defined in the MSDS (Pace Technologies, 2013). The procedure for etching with this etchant is to immerse the sample for a few seconds and rinse. Each sample was put through this process and examined under an optical microscope.

3.4 Scanning Electron Microscope Examination

A scanning electron microscope was chosen as a next step in the investigation to gain higher resolution than the optical microscope could provide. Viewing grain structure, voids and determining grain size were of interest along with distinguishing multiple phases, if possible.

The samples were repolished and coated with a gold-palladium coating to increase surface conductivity. The microscope used in this investigation was a Zeiss Ultra-55 SEM. Secondary electron and backscatter electron imaging were utilized in the investigation.

3.5 X-Ray Diffraction Investigation

X-ray diffraction is crystalline material analysis tool used to determine atomic arrangement of a material. In this study it was used to verify and quantify the phases in the samples. 15-5 PH is conventionally of martensitic structure, meaning that the lattice structure is body centered cubic (BCC) and is supersaturated with alloying elements. This supersaturation creates lattice distortions and stresses that strengthen the alloy by hindering dislocation movement. In addition, the alloy is also strengthened when the heat treatment process is applied. The process allows some of the supersaturated elements to nucleate to controlled sizes and cause a microstructure distortion and a semi-coherent lattice mismatch, further obstructing dislocation movement. This secondary phase is very small in quantity but is finely dispersed throughout the alloy.

The X-ray diffractometer used in this investigation was a Rigaku Bragg-Brentano X-ray diffractometer. The manufacturer recommended settings were used. A step size of 0.05° and a dwell time of 8 seconds were used to provide clear enough resolution and statistical significance, respectively.

X-ray diffraction was performed to verify the fully martensitic structure of each of the alloys with all heat treatments. Quantification was performed by a simplified *JADE* software, and by a completely analytical method (Materials Data Incorporated, 2011).

3.5.1 *JADE* Software Phase Quantification Method

The *JADE* software calculation uses the equation given below.

$$\%RA = \frac{A_{au} \times 0.572}{(A_{au} \times 0.572) + A_{fe}} \; x \; 100 \tag{3}$$

Where %RA is volumetric percent of the austenite phase, A_{au} and A_{fe} are the integrated area under the austenite and martensite/ferrite peaks, respectively, of the experimentally obtained X-ray diffraction curve. The factor of 0.572 is the scattering correction factor provided by the software without explanation. The factor seemed to be for a general case and not necessarily for this particular case, therefore a more complex analytical method was derived.

3.5.2 Analytical Method

The *JADE* software method and its simplistic correction factor did not seem to include many variables that should be accounted for in such a complex physical setup. Research into standards for the setup led to a derived analytical calculation, based on the direct comparison method, accounting for many variables in the experiment to achieve more accurate measurements. Using *ASTM E975 – 13 X-Ray Determination of Retained Austenite* and *Elements of X-Ray Diffraction* by Cullity as resources, a formula used to determine the volume of retained austenite was derived as described below (ASTM International, 2013) (Cullity, 1956).

The integrated intensity per angular diffraction peak, $I_\alpha{}^{hkl}$, in the α'-phase is measured by the X-ray diffractometer and is also defined below for theoretical background. Note that in these equations the α'-phase and the α-phase correspond to the martensite and ferrite phases, respectively, and are used interchangeably to represent the BCC structure.

$$I_\alpha^{hkl} = \frac{K R_\alpha^{hkl} V_\alpha}{2\mu} \tag{4}$$

Where:

I_α^{hkl} = Integrated intensity per angular diffraction peak (hkl) in the α-phase,

μ = Linear absorption coefficient for the steel,

V_α = Volume fraction of the α-phase

And,

$$K = \frac{I_o e^4 \lambda^3{}_A}{32\pi r m^2 c^4} \tag{5}$$

Where:

I_o = Intensity of the incident beam,

e, m = Charge and mass of an electron,

r = Radius of the diffractometer,

c = Velocity of light

λ = Wavelength of incident radiation,

And

$$R_\alpha^{hkl} = \frac{1(/F/^2 p LP e^{-2M})}{v^2} \tag{6}$$

Where:

v = Volume of the unit cell,

$/F/^2$ = Structure factor times its complex conjugate,

p = Multiplicity factor of the (hkl) reflection,

LP = Lorentz Polarization factor for a monochromator setup,

e^{-2M} = Debye-Waller or temperature factor

And

$$LP = \frac{(1 + \cos^2 2\alpha \cos^2 2\theta)}{\sin^2 \theta \cos \theta} \tag{7}$$

For a monochromator setup, where:

θ = Bragg angle

2α = The diffraction angle of the monochromator crystal

And

$$M = \frac{B sin^2\theta}{\lambda^2} \tag{8}$$

Where:

$$B = 8\pi^2 \mu_s{}^2 \tag{9}$$

Where:

$\mu_s{}^2$ = The mean square displacement of the atoms from their mean position, in a direction perpendicular to the diffracting plane

And

$$\frac{I_\alpha{}^{hkl}}{I_\gamma{}^{hkl}} = \left(\frac{R_\alpha{}^{hkl}}{R_\gamma{}^{hkl}}\right)\left(\frac{V_\alpha}{V_\gamma}\right) \tag{10}$$

And

$$V_\alpha + V_\gamma = 1 \tag{11}$$

Thus:

$$V_\gamma = \frac{(I_\gamma/R_\gamma)}{\left[(I_\alpha/R_\alpha) + (I_\gamma/R_\gamma)\right]} \tag{12}$$

This method assumes that only austenite (γ) and martensite (α') phases are present and all crystals are randomly oriented. Carbide phases are excluded from the equation because carbon composition is limited to very low amounts such that carbide phases were not detected during experimental X-ray diffraction runs.

3.6 Transmission Electron Microscopy

Transmission electron microscopy was utilized in an attempt to locate other minor phases within the microstructure of the samples at a greater resolution than the SEM could provide. The location of phases within the microstructure could potentially hold clues regarding formation and associated properties.

3.6.1 Focused Ion Beam Milling

The focus ion beam (FIB) (FEI ™ 200TEM) in-situ lift-out (INLO) technique was employed to prepare transmission electron microscopy (TEM) specimens. In FIB-INLO, a high-energy beam of focused Ga^+ is employed for imaging and milling. A thin Pt layer was deposited first to the surface of the selected area so as to protect the region of interest. Then two trenches were cut below and above the Pt layer. The bottom part was further cut completely while parts of the sides were left attached. Then, the W-needle, which is welded to the specimen by using Pt, is used to pick up the specimen. The specimen is typically wedge shaped and mounted to a 3mm diameter copper grid. The specimen is further thinned to a final thickness of less than 200nm, suitable for TEM/STEM analysis.

3.6.2 Transmission Electron Microscope Analysis

A Philips/Tecnai ™ F30 300K eV TEM, equipped with a Fischione ™ high angle annular dark field (HAADF) and energy dispersive X-ray spectroscopy (EDS) was employed to examine the microstructure and phase constituents of the specimen. Crystallographic phase identification of the phases was performed using selected area diffraction (SAD)

methods. Diffraction ring patterns from different areas were obtained and used to check the retained austenite phase within the martensite.

3.7 Energy Dispersive X-Ray Spectroscopy

A method used take semi quantitative measurements of elemental composition of a material is energy dispersive X-ray spectroscopy (EDS). An electron beam is accelerated toward a sample in a vacuum. The beam excites atoms in the sample which then emit X-rays. The energies of these X-rays are characteristic to each type of atom and are collected by a detector and analyzed by software. Elements of low atomic number are not accurately quantified. A DMLS sample and a conventional sample were analyzed using this method.

3.8 Glow Discharge Atomic Emission Spectrometry

Glow discharge atomic emission spectrometry was carried out by SGS MSi based in Melrose Park, IL. This type of analysis is also referred to as LECO ™ analysis as it was commercialized by the LECO ™ Corporation. The process involves sputtering atoms from the surface of a sample using a stream of argon gas ions in a low pressure atmosphere. Sputtered atoms from the sample flow with the argon gas stream through an atomic emission spectrometer which detects the frequency and intensity of the emitted photons. The frequency is used to identify the type of atom detected and the intensity corresponds to the amount of the element in the sample based on a standard.

Three samples were sent out to the vendor for analysis including DMLS recycled powder, DMLS 15-5PH as-sintered without heat treatment, and a sample of conventional 15-5PH in the annealed condition. The process was performed according to ASTM E1019-

11 *Standard Test Methods for Determination of Carbon, Sulfur, Nitrogen and Oxygen in Steel,*

Iron, Nickel and Cobalt Alloys by Various Combustion and Fusion Techniques and is accurate

for a nitrogen range of 0.0010 to 0.5wt% (ASTM International, 2011).

CHAPTER 4: RESULTS AND ANALYSIS

4.1 Microstructure

4.1.1 Optical Microscopy

The optical micrographs of the microstructures of all samples in this study are shown in **Figure 4** and **Figure 5**.

The low magnification optical images in **Figure 4** shown the layering effect that occurs on the heat treated DMLS samples (c), (e) and (g). This effect is not observed in the conventional alloy samples or in the as-sintered (not heat treated) sample in (a).
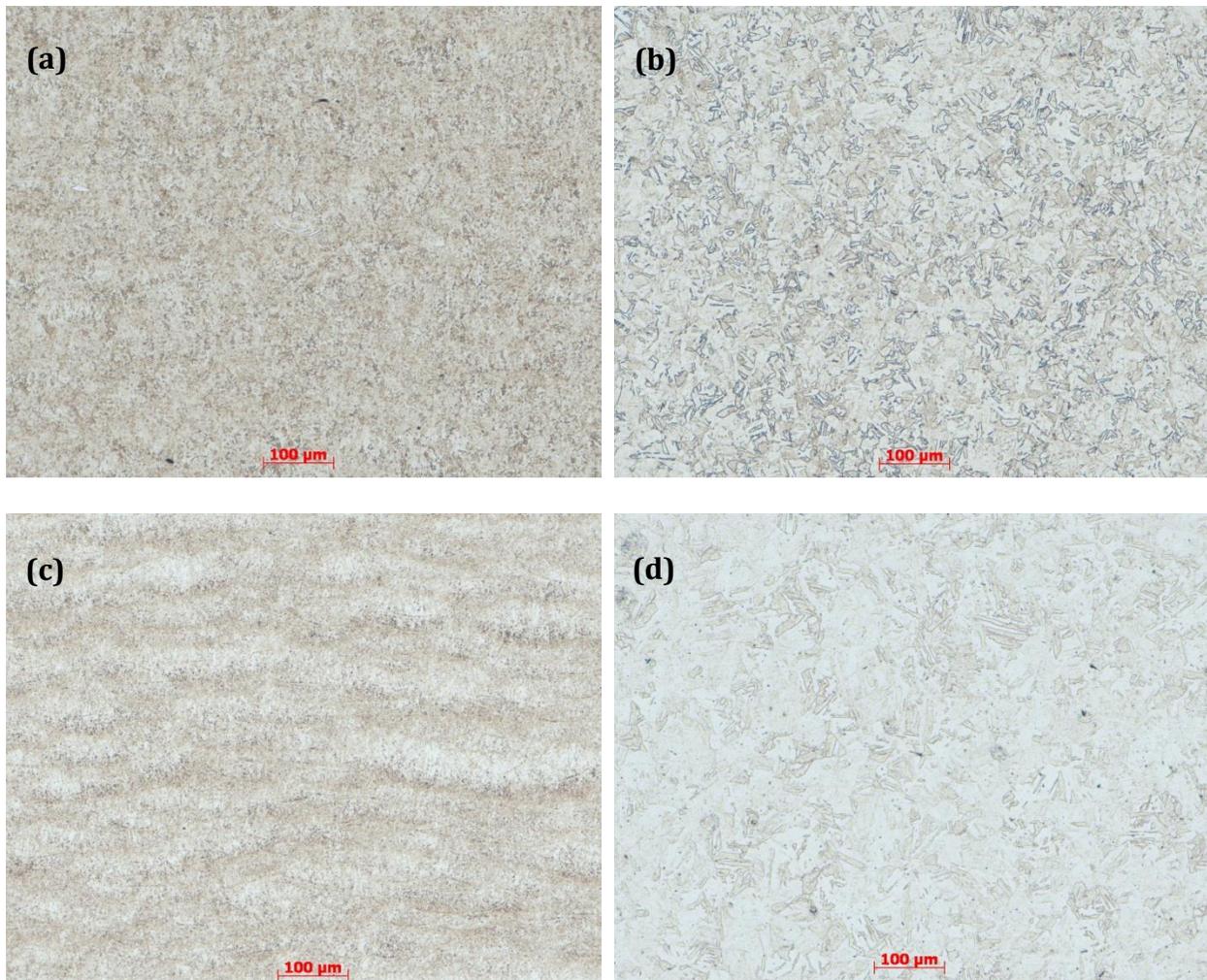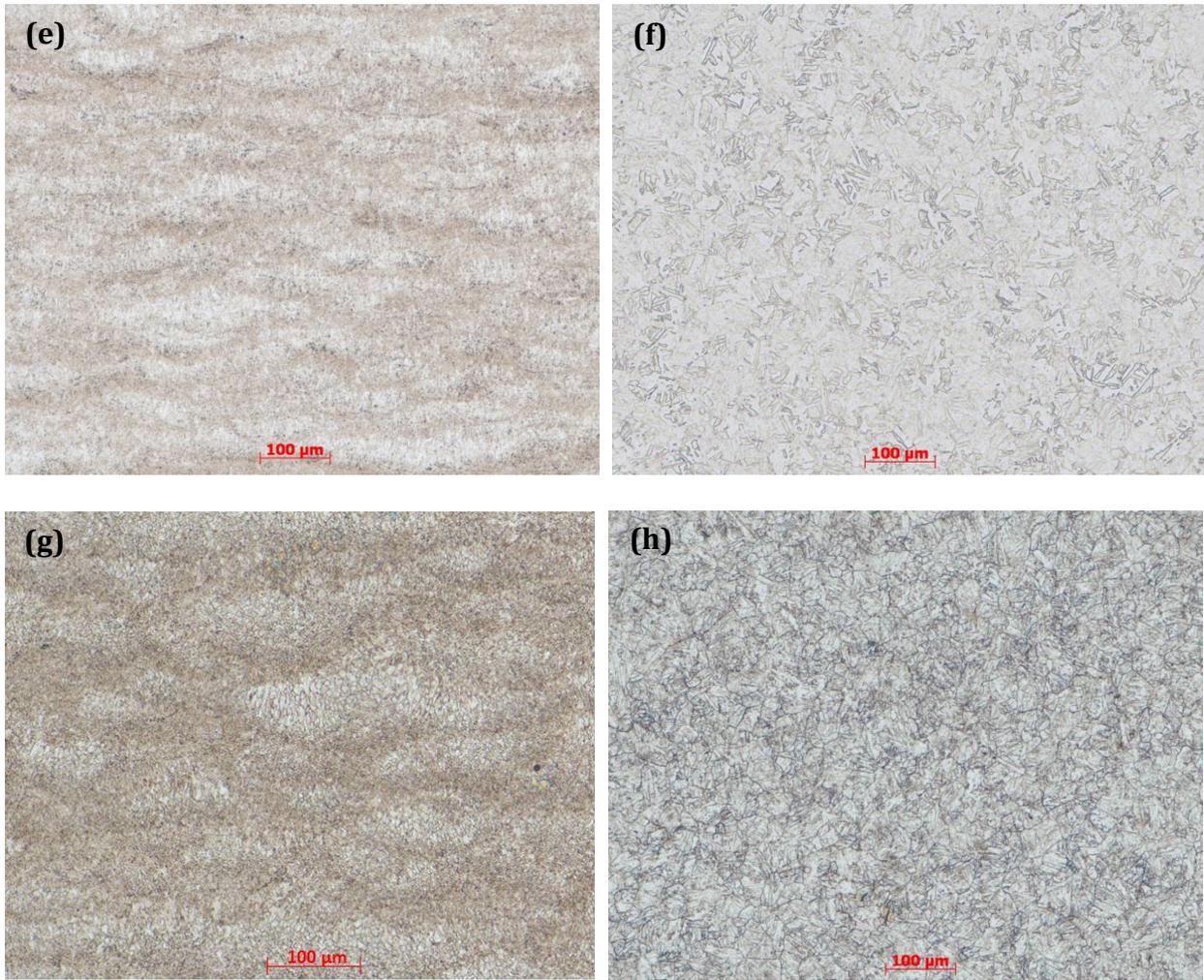
Figure 4: Low Magnification of Microstructure:

(a) DMLS alloy – no heat treatment. (b) Conventional alloy – no heat treatment. (c) DMLS alloy – LH900 heat treatment. (d) Conventional alloy – H900. (e) DMLS alloy – LH1025 heat treatment. (f) Conventional alloy – H1025. (g) DMLS alloy – LH1150 heat treatment. (h) Conventional alloy – H1150.

In **Figure 5**, the prior austenite grain boundaries were revealed by Vilella's reagent. These grain boundaries can be used to determine grain size, which often correlates with mechanical properties. Prior austenite grain size calculations were performed using the planimetric procedure as described in ASTM E112-13 (ASTM International, 2013). The ASTM grain size of the prior austenite grains of the conventionally processed alloy was 7 to 7.5, which corresponds to an average diameter of 31.8µm to 26.7µm, respectively. The distinguishable sections within each layer of the DMLS processed alloy were measured and

the ASTM grain size of the prior austenite grains was 11.5 to 12, which corresponds to an average diameter of 6.7µm to 5.6µm, respectively. The DMLS grain size calculation accounts for distinguishable grains revealed by the etchant. Other grains were relatively smaller and did not display distinguishable prior austenite grain boundaries. It should also be noted that the calculations assume an equiaxed grain structure. This is fairly representative of the prior austenite grains in the conventionally processed alloy, as shown in **Figure 5** (i). However, the DMLS processed alloy exhibits a layered structure displaying similar characteristics of cast ingot grain structure on a very fine scale as shown in **Figure 5** (h). These similar characteristics are shown in **Figure 6**. Each layer of sintered metal displays a microstructure of very fine grains at the bottom of the layer, followed by elongated columnar grains, leading to generally equiaxed grains. After the layer of equiaxed grains, the pattern is repeated as shown in **Figure 4** (g).
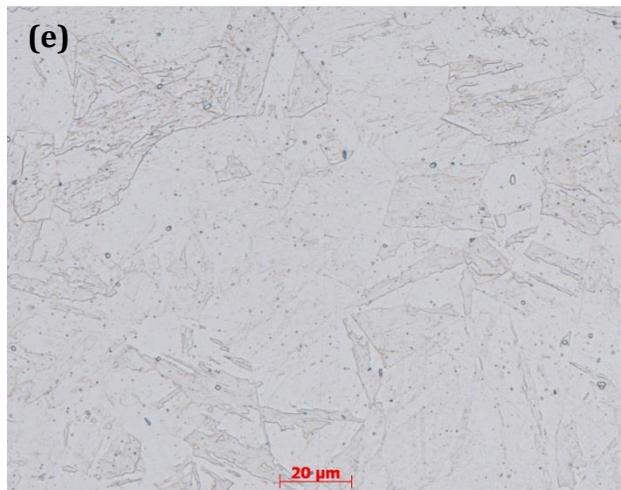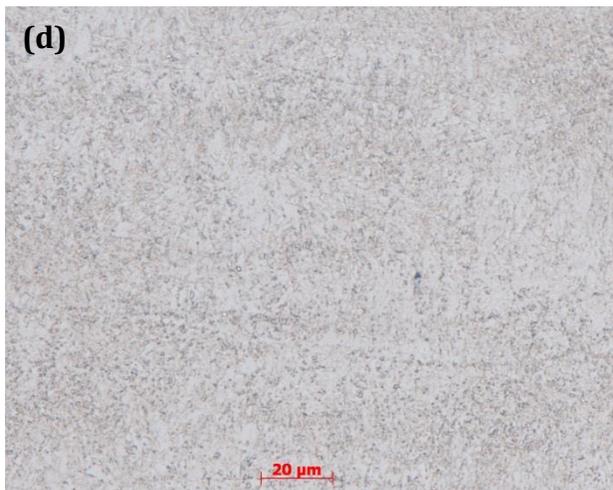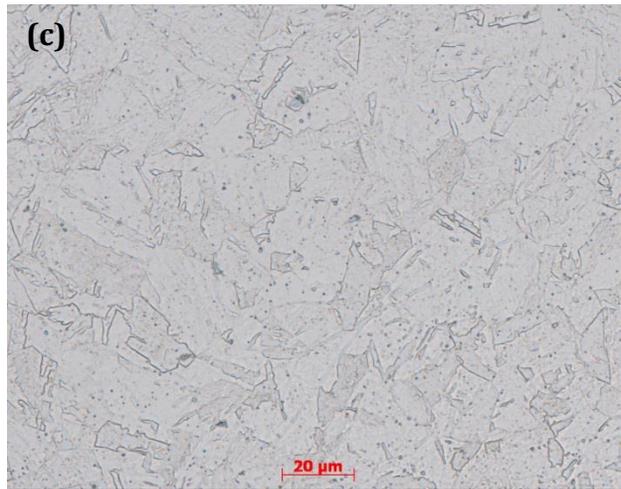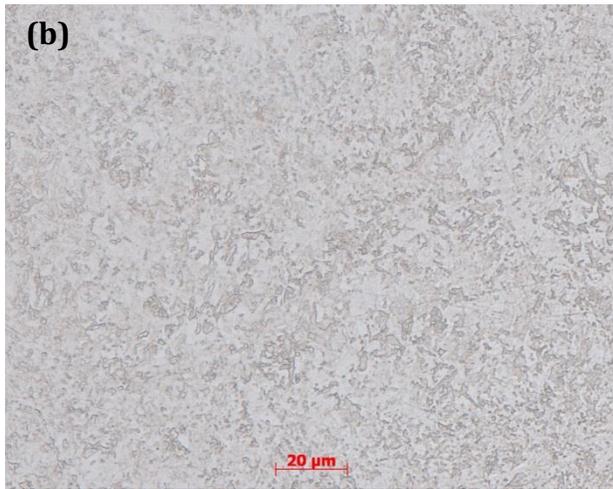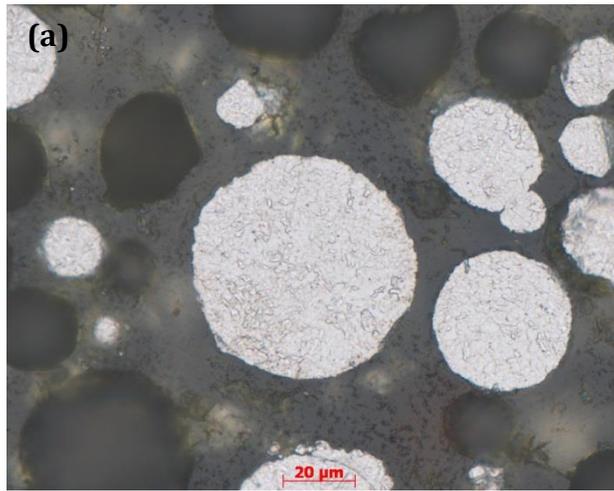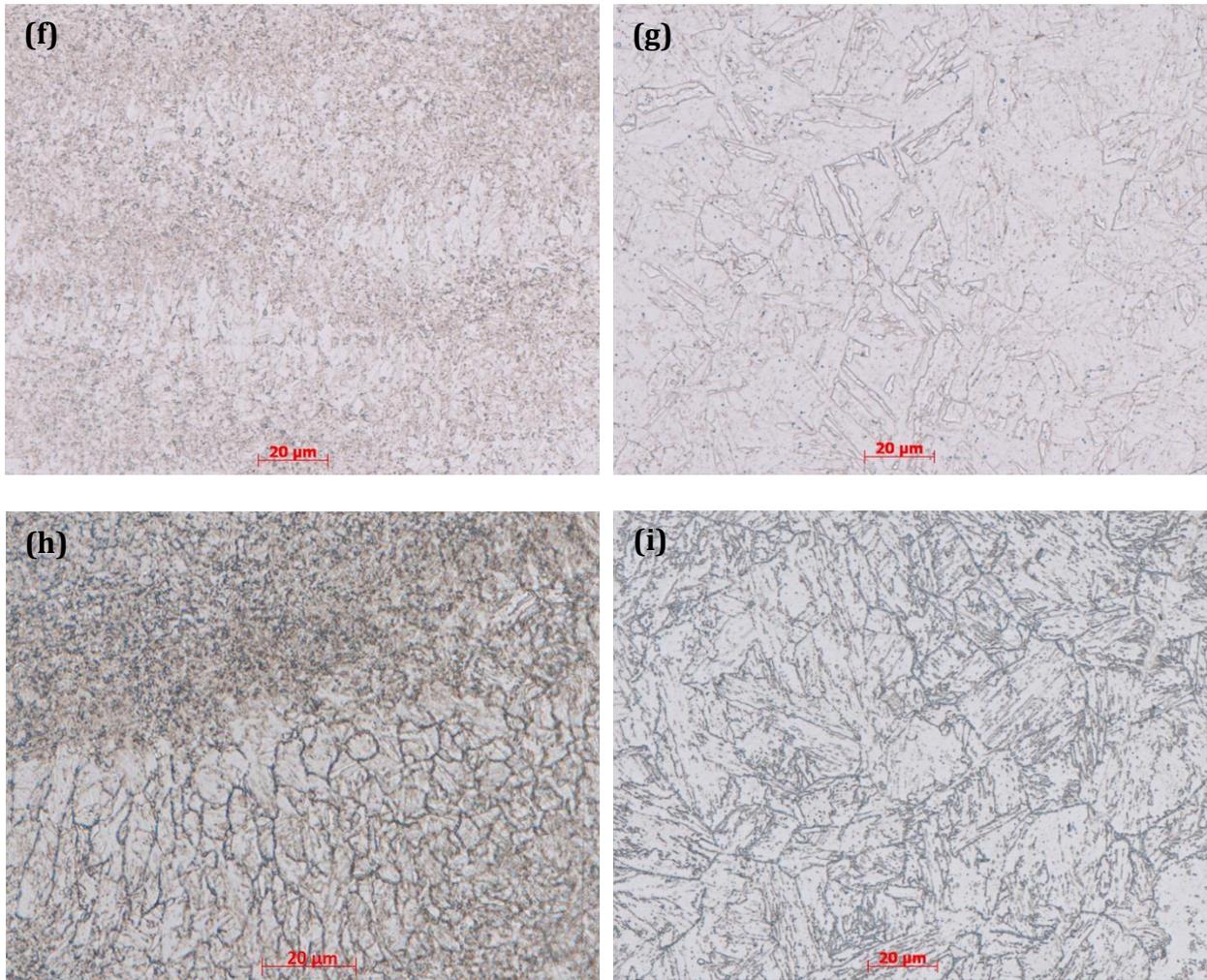
Figure 5: High Magnification of Microstructure:

(a) Unsintered DMLS powder particles. (b) DMLS alloy – no heat treatment. (c) Conventional alloy – no heat treatment. (d) DMLS alloy – LH900 heat treatment. (e) Conventional alloy – H900. (f) DMLS alloy – LH1025 heat treatment. (g) Conventional alloy – H1025. (h) DMLS alloy – LH1150 heat treatment. (i) Conventional alloy – H1150.
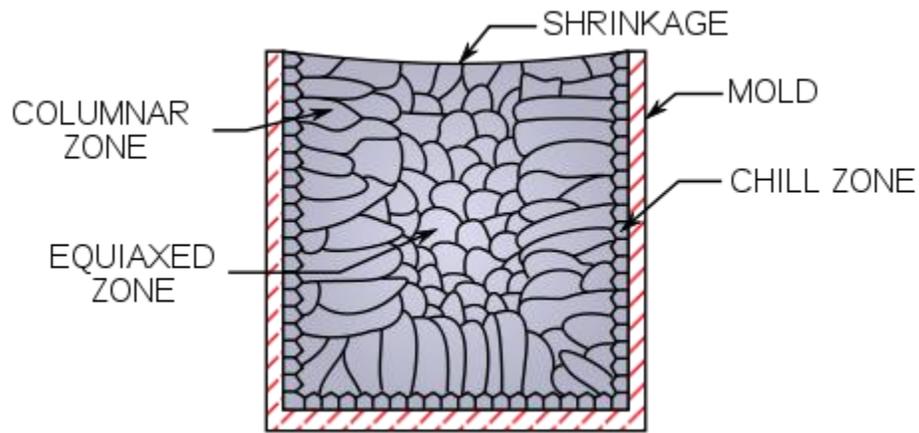
Figure 6: Cast Ingot Grain Structure (Cdang - Original Work, 2009)

4.1.2 Scanning Electron Microscopy

Powder particles were observed via SEM. **Figure 7** (a) displays a representative variety of particle shapes and sizes. Some satellite particles are attached to larger particles and may have formed either during cooling of the powder during gas atomization or from residual heat from previous DMLS processing of the recycled powder. **Figure 7** (b) shows a few particles that have been ground and polished. Voids and/or pull-outs can be seen within the particles.
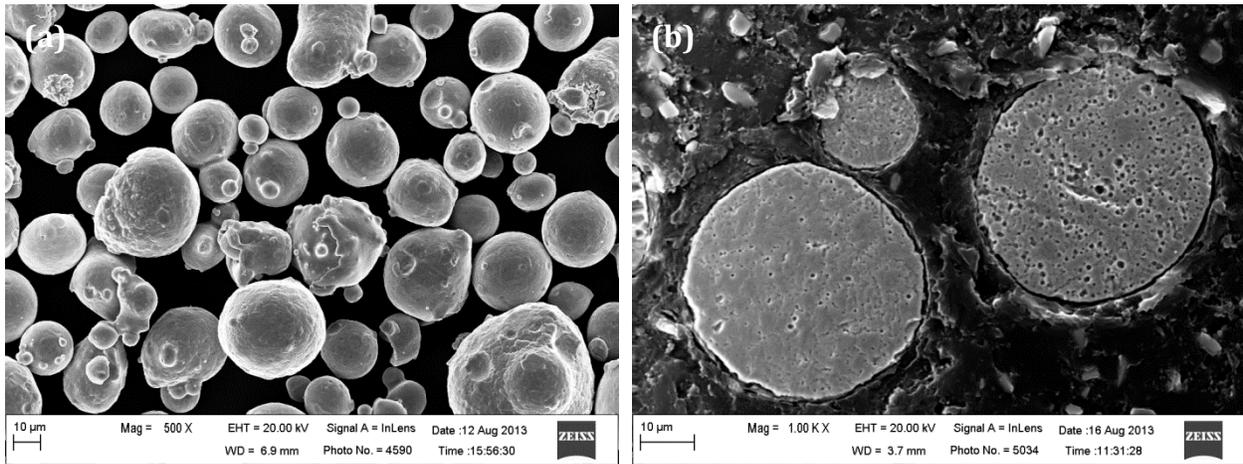
Figure 7: Powder Particles:

(a) Powder particles of a variety of shapes and sizes. (b) Ground and polished particle cross-sections.

4.1.3 Transmission Electron Microscopy

A typical bright field martensitic lath structure from the DMLS LH1025 sample is shown with the corresponding selected area diffraction pattern (SADP) in **Figure 8**.
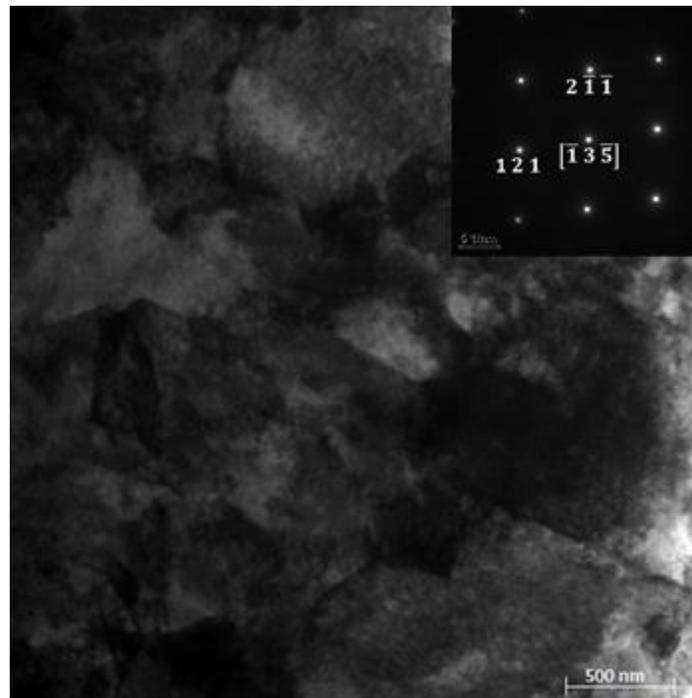
Figure 8: Bright field micrograph of lath martensite with selected area diffraction pattern.

The TEM image in **Figure 9** (a) shows a martensitic structure and (b) shows the corresponding SADP. The nearly ring pattern identifies strong martensitic BCC rings and also shows faint signs of austenitic FCC diffraction as pointed out by arrows on the micrograph. The arrow on the inner ring corresponds to the FCC (200) plane and the arrow pointing to the outer ring corresponds to the FCC (220) plane. Although faint, the spots in these locations prove the existence of relatively small retained austenite grains within the martensite matrix.
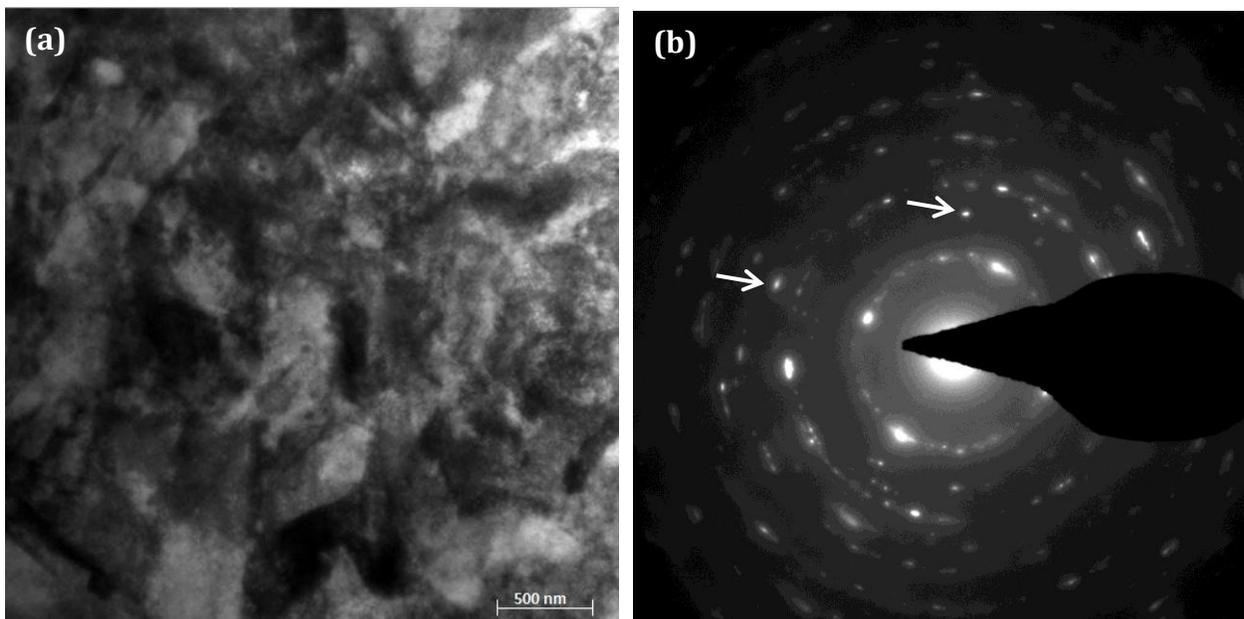
Figure 9 : Martensitic lath structure with retained austenite:

(a) Martensitic structure. (b) Corresponding ring pattern showing presence of austenite.

4.2 Phase Evolution

XRD scan results from the DMLS samples are shown in **Figure 10**. Each set of data is offset by 500 counts to reduce overlapping for visual effect. The data peaks are labeled as BCC or FCC along with their respective plane of reflections. The integrated areas under

these peaks were used in the calculation of phase fraction reported in **Table 4.** These phase

fractions were calculated using equations (4) through (12) in section 3.5.2.

Table 4: Analytical Austenite Phase Calculation Results

Sample	Percent Austenite (Vol. %)	Standard Deviation (Vol. %)
DMLS Recycled Powder	4.96	1.25
DMLS No Heat Treatment	7.52	1.70
DMLS LH900	9.05	2.34
DMLS LH1025	5.57	1.23
DMLS LH1150	13.06	2.98
Conventional Annealed	0.00	N/A
Conventional H900	0.00	N/A
Conventional H1025	0.00	N/A
Conventional H1150	3.68	0.75
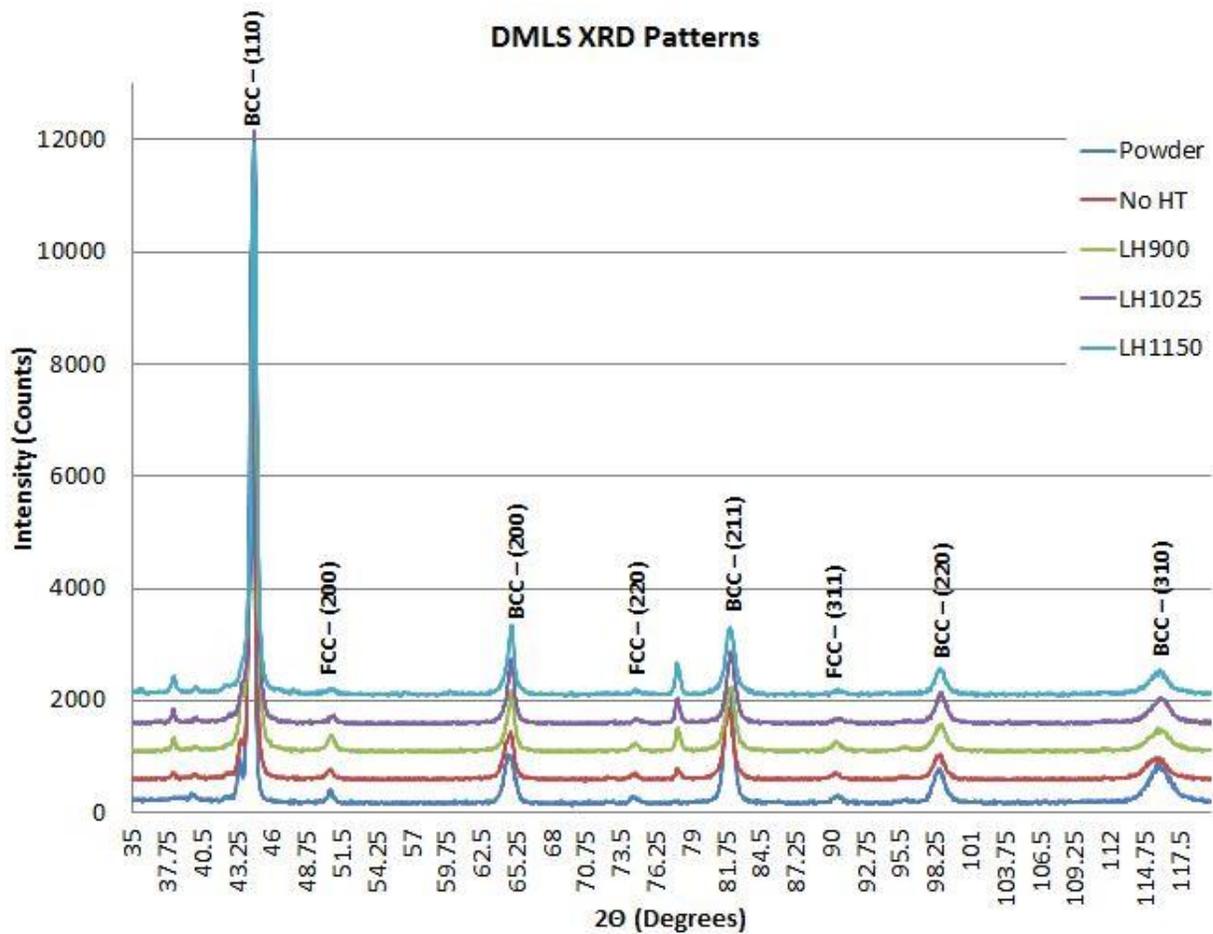
Figure 10: DMLS XRD Phase Variation with Heat Treatment

XRD scan results from the conventional samples are shown in **Figure 10**. Each set of data is offset by 500 counts to reduce overlapping for visual effect. The lack of significant FCC peaks corresponds to an absence of retained austenite.
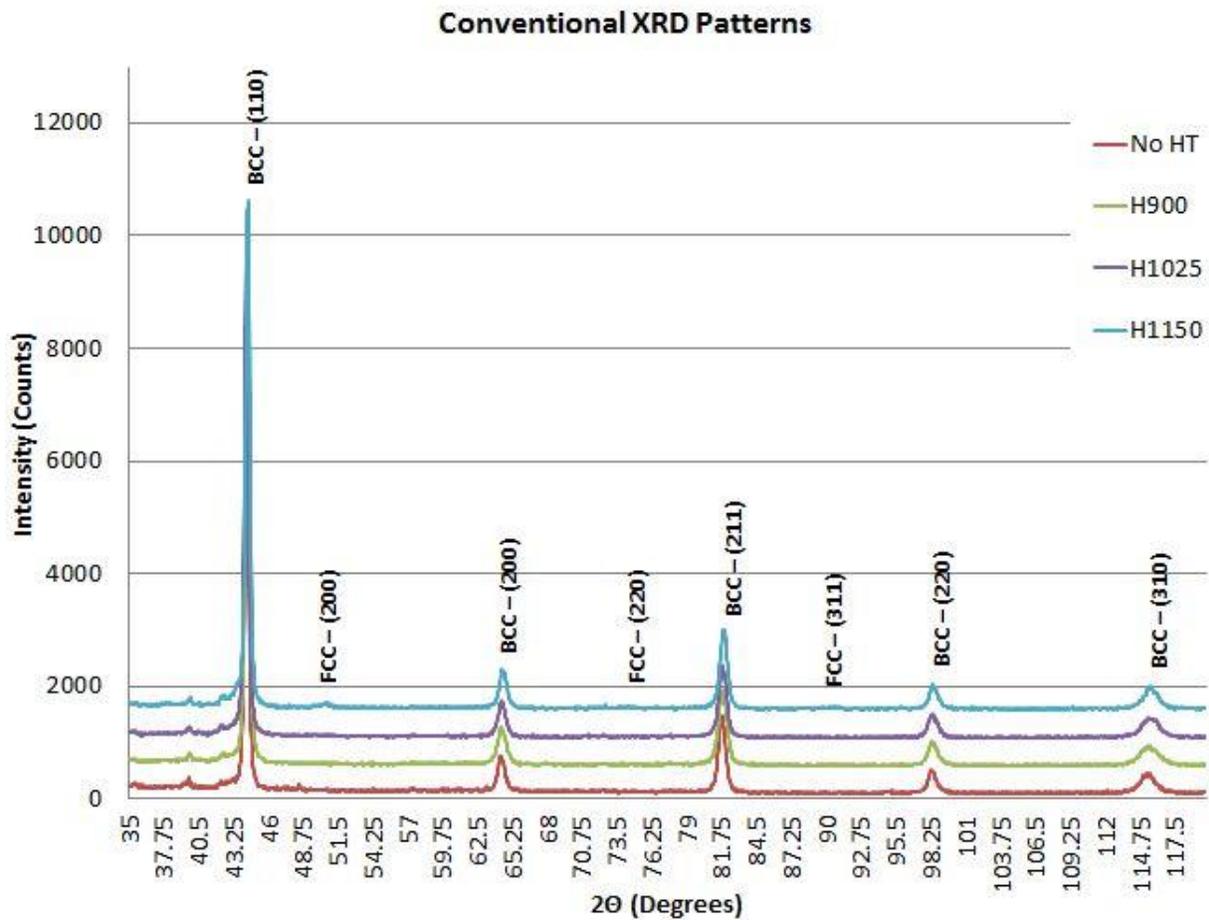
Figure 11: Conventional XRD Phase Evolution

The volume percent of the austenite phase was calculated according to the

analytical procedure described in section 3.5.2. The trend in retained/reverted austenite

for each set of samples is shown in **Figure 12**. The results of the analytical calculations,

including standard deviation, are given in **Table 4**. Each sample was scanned at least three

times in the X-ray diffractometer to achieve statistically significant results. The trend in

Figure 12 shows an increase in austenite phase in the DMLS samples with more processing

and higher temperature heat treatments with this exception of a reduction of austenite in

the H1025 heat treatment when compared to the amount of austenite in the as-sintered

DMLS sample.
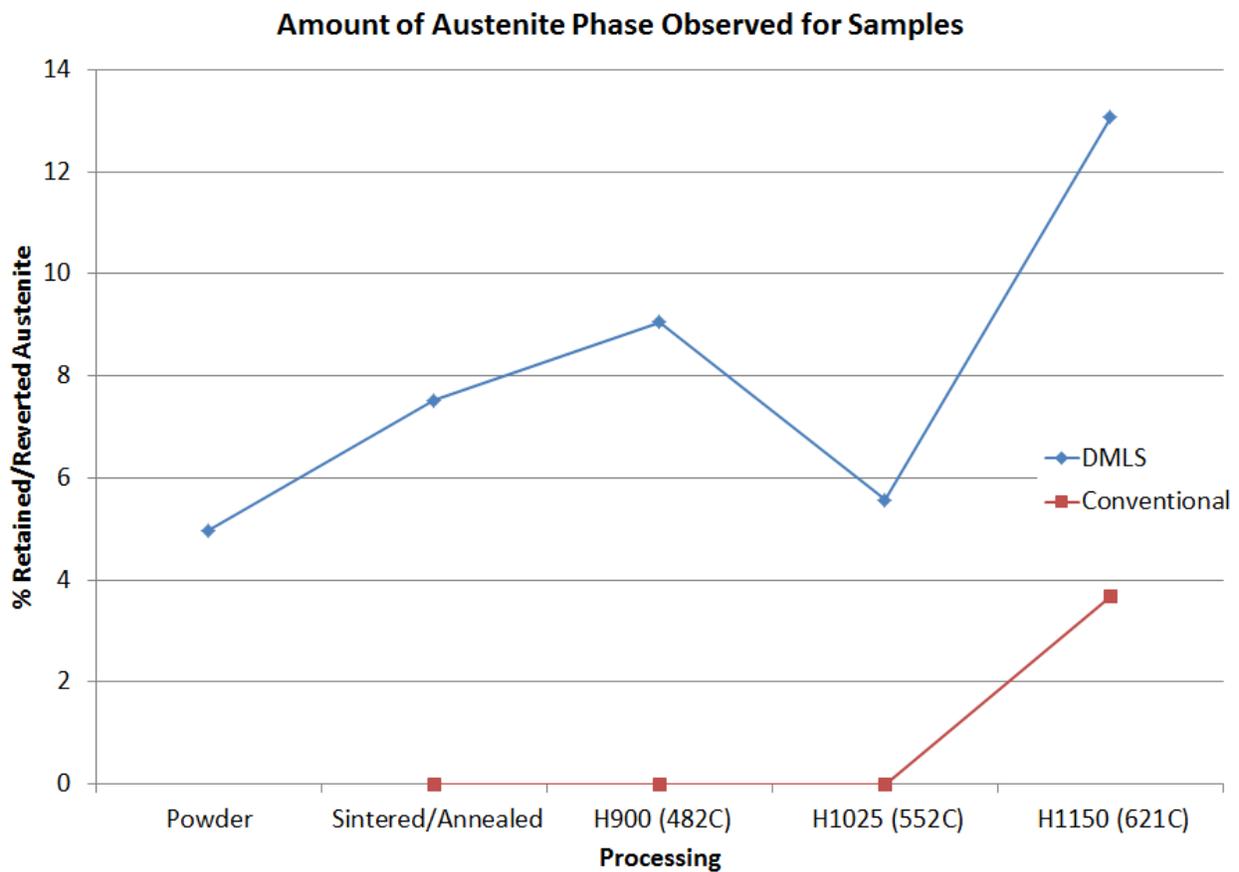
Figure 12: Amount of Austenite Phase Observed for Samples

4.3 Compositional Differences

Upon discovery of the reduction in austenite in the DMLS LH1025 heat treatment in comparison to the as-sintered DMLS sample, the composition of the sample sets were checked for conformance using the semi-quantitative method of energy dispersive X-ray spectroscopy (EDS). All samples were confirmed to meet UNS S15500 specifications on all elements with larger atomic number than oxygen, since EDS is not very accurate with elements with atomic number smaller than oxygen (ASTM International, 2013). A compositional difference of additional impurities outside of the specified elements was a possibility, and given that most of the DMLS processing had taken place in a nitrogen gas

environment, there was a good chance of finding higher nitrogen values in the DMLS

samples than in the conventionally processed alloy.

This reasoning led to the decision to perform GDS to determine the nitrogen content

of the DMLS powder, a DMLS sample without heat treatment, and a conventionally

processed sample in condition A, the annealed state. This type of analysis is also referred to

as LECO ™ analysis as it was commercialized by the LECO ™ Corporation. The results of the

GDS nitrogen analysis are given in **Table 5** and clearly show that significant nitrogen

content has been added to the DMLS powder and retained through the build process.

Table 5: Glow Discharge Atomic Emission Spectrometry Nitrogen Analysis Results

Sample	**Nitrogen (wt%)**	**Standard Deviation (wt%)**
DMLS Recycled Powder	0.11	0.001514
DMLS As-sintered	0.080	0.0002066
Conventional No Heat Treatment	0.019	0.0004293

CHAPTER 5: DISCUSSION

5.1 Microstructural Development

The DMLS microstructure differs from the conventionally processed 15-5PH microstructure because of the layering effect and distribution of smaller grain sizes. The conventional alloy has an equiaxed prior austenite grain structure but the DMLS grain structure cycles between relatively small grains and elongated larger grains. This is likely due to the rapid cooling rate that laser sintering causes. Such a high temperature for melting over a relatively shallow depth of the melt pool would induce this rapid cooling effect and contribute to elongated grains in the direction of heat flow out of the melt pool. Rapid cooling would also refine the grain size due to a lack of time for grain growth upon solidification prior to diffusion becoming limited by lower temperatures. Some of the expected elevated mechanical properties of the DMLS alloy can be attributed to this unique, large and small grain layered structure and anisotropic behavior with respect to the part build direction. Both of the DMLS and the conventionally processed alloys martensitic grain structures have a similar lath structure expected of a high alloy, low carbon steel.

TEM analysis confirmed the presence of the austenite phase within the martensite matrix but location of the retained austenite grains could not be identified.

The cross section of the powder particles revealed voids or gas pockets caused by either entrapment of the nitrogen gas or off-gassing during gas atomization of the powder. Both mechanisms would likely contribute to the high nitrogen levels in the alloy determined by GDS.

5.2 Phase Evolution

The retained austenite is a major issue in the DMLS 15-5PH. The results given in **Figure 12** indicate a general increasing trend with increasing heat treatment temperature with a reduction in the austenite phase for the LH1025 heat treatment compared to the DMLS as-sintered sample. A hypothesis for this decrease in austenite phase for the LH1025 heat treatment is that secondary phases including carbides, nitrides and copper-rich precipitates may preferentially form in the grain boundaries or within the retained austenite where the activation energy is relatively lower than within the martensite matrix. Precipitate formation would use local elemental resources from the surrounding grains. This may be caused by the free energy barrier for diffusion being lower in the more homogeneous, softer austenite grains at lower heat treatment temperatures than within the harder, supersaturated martensite lath. Once higher temperatures are reached, such as seen in the LH1150 heat treatment, free energy increases in the martensitic matrix and an additional reverting of some martensite occurs in reverse via diffusionless transformation as the temperature approaches the reaustenization temperature. This additional effect of reverted austenite was observed and calculated to be 3.68 vol. % in the H1150 heat treatment in the conventionally processed sample. This reverting of the martensite phase into austenite was also observed by Bajguirani with aging of 15-5PH at temperatures above 600°C (1112°F) (Bajguirani, 2002).

An alternative theory for the existence of retained austenite in the DMLS samples involves a shift in the martensite start and finish temperatures. These temperatures are known to fluctuate with alloy content (ASM International, 2005). Generally with higher alloy content, the temperatures shift to lower values. This means that it is very likely that additions of strong austenite formers like nitrogen or other impurities may lower the

martensite start, and more importantly, the martensite finish temperature lower than the

specified final cooling temperature in the heat treatment specification of 90°F (32.2°C) and

possibly lower than room temperature leaving some austenite untransformed.

AMS2759/3E specifies that the alloy should be air-cooled to 90°F (32.2°C) within one hour

of heat treating (ASM International, 2005). Additionally, it should be noted that the build

chamber temperatures may be greater than 90°F (32.2°C) for the duration of building the

part, preventing full martensitic transformation from taking place.

5.3 Compositional Comparison

The compositions of the DMLS and the conventionally cast 15-5PH both fall within

the specifications of ASTM A564 (ASTM International, 2013). The main difference between

the compositions is the difference in nitrogen content, which is a known strong austenite

former. Nitrogen behaves similar to carbon in steels, which is deemed very detrimental to

this alloy and thus is limited to 0.07 wt%. With low carbon content, nitrogen has space to

migrate to interstitial sites within the iron-based alloy.

The effect of the austenite formers, including nitrogen, and martensite/ferrite

formers has been studied and quantified by Schaeffler and Long et al. among others

(Schaeffler, 1949) (C. J. Long, 1973) (ASM International, 2005). The equations (1) and (2)

given in section 2.3.2 account for influence of the austenite and martensite/ferrite forming

elements on the microstructure. Putting maximum and minimum compositional values into

the equations will outline a range of phase constituent possibilities for this alloy as shown

in **Figure 13**. The calculated nickel equivalent range representing austenite formers is 4 to

8.1. The calculated chromium equivalent range representing martensite/ferrite formers is

15.575 to 17.225. The calculation was repeated for the austenite forming equation but with

the inclusion of nitrogen and as a result, the equivalent nickel range was increased to 4.57

to 11.4. The ranges without accounting for nitrogen are visually outlined by the dark blue

box, and the ranges accounting for nitrogen content are outlined in orange. The addition of

nitrogen causes a vertical shift of the range upward, more into the austenite region.
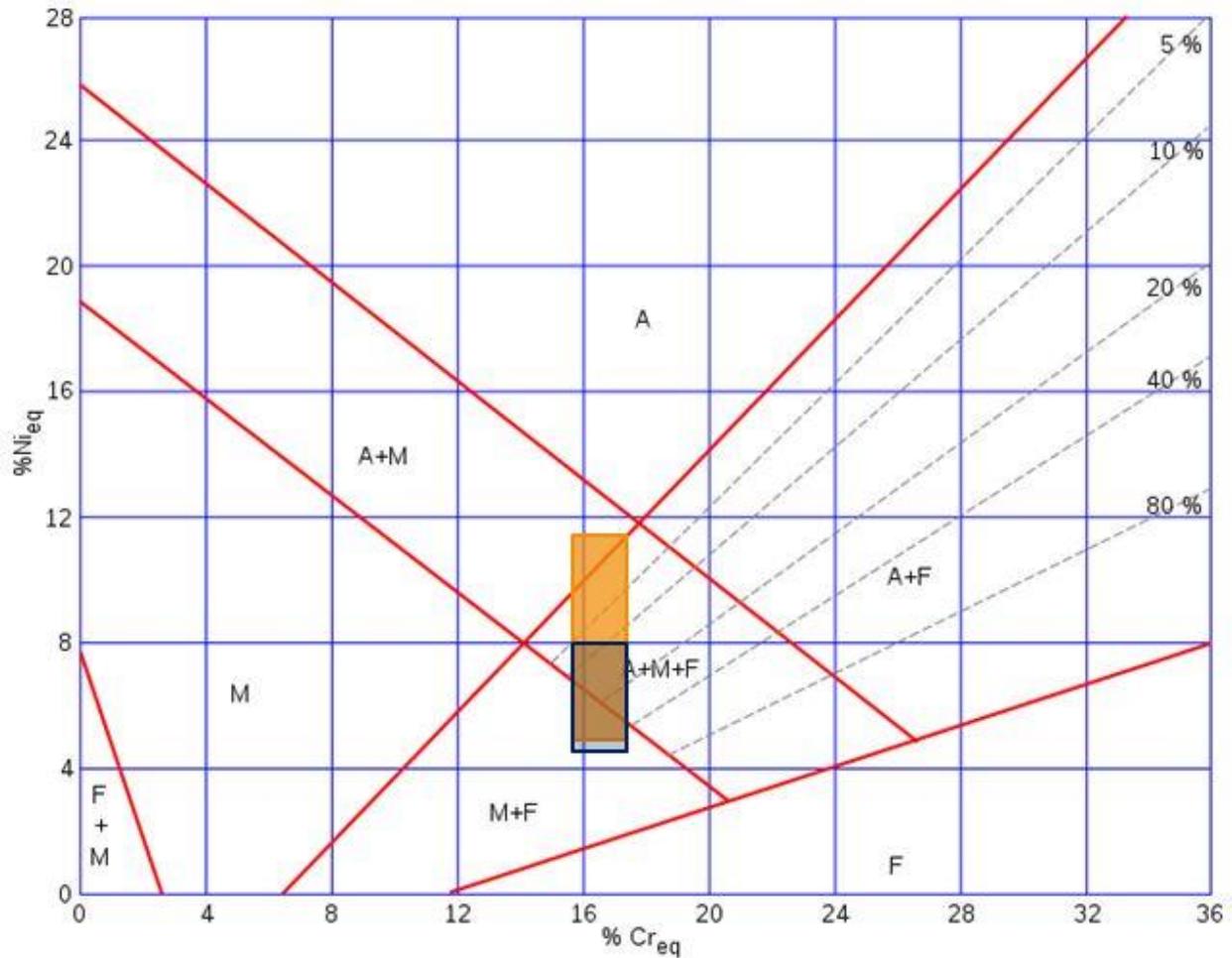
Figure 13: Calculated Phases Applied to Schaeffler Diagram:

Dark blue box represents 15-5PH range without nitrogen. Orange box represents 15-5PH
range with nitrogen.

5.4 Suggested Processing Improvements

Based on the results of this study some DMLS process improvement changes are suggested. Three methods can be used separately or in combination to reduce the retained/reverted austenite.

First, a post-build and post-heat treatment air cool to a temperature well below 90°F (32.2°C), should be considered. This will cool the part to a temperature well below the martensite finish temperature and allow for full transformation to take place. The second suggestion is to produce 15-5PH powder with low nitrogen content by utilizing inert argon gas as opposed to nitrogen for gas atomization. Other austenite and martensite/ferrite forming elements can be more tightly controlled to be on the lower side of the specified range in order to fall on the martensite side of the austenite-martensite line in Schaeffler diagram in **Figure 13**. In addition, the DMLS build processing should also take place under an argon atmosphere so that no nitrogen is added during laser sintering. Removal of the nitrogen should remove all retained austenite content, similar to the conventionally produced alloy. However, the H1150 heat treatment is not recommended with this method due to the formation of reverted austenite. The last process improvement method is to perform the standard heat treatment, including the annealing step as specified in *AMS 2759/3E* (SAE International, 2008), as opposed to the manufacturer recommendations to skip the annealing step. Annealing the DMLS part will allow for proper cooling and eliminate the delayed cooling history of the heated build chamber. This step will also change the grain structure to be more similar to the conventionally cast samples. The future applications of any of these suggestions would be valuable follow-up research to this study.

CHAPTER 6: SUMMARY AND CONCLUSIONS

The microstructure phase constituents and chemistry of DMLS 15-5PH has been investigated and the findings reveal some challenges and room for process improvement. DMLS 15-5PH, compared to its conventionally processed counterpart, has a smaller grain size along with a layered microstructure. This is suggestive of anisotropic and elevated strength but with lower ductility. The main challenge discovered upon investigation is the lack of full martensitic transformation due to retained/reverted austenite.

The austenite phase fraction was quantified for DMLS and conventionally processed samples through multiple heat treatments. A significant contributor to this unwanted austenite phase is the high nitrogen content in the alloy which is likely absorbed during the nitrogen gas atomization process to produce the DMLS powder and retained during laser sintering in a nitrogen atmosphere. Nitrogen is a strong austenite phase former in stainless steels and will lower the martensite start and finish temperatures. The magnitude of the temperature change is a topic that requires further study.

Possible solutions to eliminate the austenite phase include adjusting the heat treatment specification for the air cooling to a temperature below the martensite finish temperature for a full martensitic transformation. Another solution would be to replace nitrogen with inert argon gas during gas atomization powder production and use argon gas in the build chamber during DMLS processing. This would eliminate nitrogen absorption in stages unique to the laser sintering process, leaving nitrogen composition comparable to that of the conventionally processed samples and thus eliminating retained austenite. A final processing solution to reduce austenite would be anneal the DMLS part prior to the precipitation hardening heat treatment. Annealing the part with proper air cooling in a

room temperature environment should reduce any austenite caused by interrupted cooling

due to elevated temperatures in the DMLS build chamber environment.

APPENDIX: PROPRIETARY INFORMATION AGREEMENT

PROPRIETARY INFORMATION AGREEMENT

THIS PROPRIETARY INFORMATION AGREEMENT, effective when last executed by a Party hereto, is made by and among LOCKHEED MARTIN CORPORATION, a Maryland corporation acting through its Missiles and Fire Control business unit having a place of business at Orlando, Florida, United States of America (hereinafter referred to as "LOCKHEED MARTIN"), and KEVIN COFFY, a UCF student and Lockheed Martin College Work Experience Program (CWEP) participant, having a place of business at Orlando, Florida, United States of America (hereinafter referred to as "COFFY") and UNIVERSITY OF CENTRAL FLORIDA, by and on behalf of its Board of Trustees, having a place of business at Orlando, Florida, United States of America (hereinafter referred to as "UCF"). COFFY and UCF may collectively be referred to as THE PARTICIPATING PARTIES; and LOCKHEED MARTIN, THE PARTICIPATING PARTIES may each or all be referred to hereinafter as a "Party" or the "Parties", respectively.

WHEREAS, LOCKHEED MARTIN possesses or may in the future possess certain technical, business, financial and other information of a proprietary nature ("Proprietary Information") specifically including information that pertains to testing of materials manufactured using an EOS 270 Directed Metal Laser Sintering machine; test results, Intellectual Property contained within disclosure MC-03503 ("Subject"); and

WHEREAS, COFFY possess or may in the future possess certain technical, business, financial and other information of a proprietary nature ("Proprietary Information") specifically including information that pertains to test results and data of Lockheed Martin's materials manufactured using an EOS 270 Directed Metal Laser Sintering machine ("Subject"); and

WHEREAS, UCF possesses or may in the future possess certain technical, business, financial and other information of a proprietary nature ("Proprietary Information") specifically including information that pertains to test results and data owned by Lockheed Martin as a result of testing at UCF's facility of materials manufactured using an EOS 270 Directed Metal Laser Sintering machine ("Subject"); and

WHEREAS, LOCKHEED MARTIN and THE PARTICIPATING PARTIES desire access to each other's aforesaid Proprietary Information solely for purposes of evaluation and/or interfacing with each other and/or each other's products and services in relation to permit a UCF student (Coffy) to share limited test data, reports, and other information in regards to a planned laboratory evaluation for a Master's Thesis as it relates to LMC IP disclosure MC-03503, after Coffy has received prior written authorization from Lockheed Martin to release outside of UCF for publication ("Purpose"); and

WHEREAS, LOCKHEED MARTIN and THE PARTICIPATING PARTIES are willing to provide each other with such required access for the above-stated Purpose under conditions preserving the proprietary nature of the Proprietary Information so disclosed;

NOW, THEREFORE, in consideration of these premises, and of the mutual promises and covenants contained herein, the Parties hereto agree as follows:

1)   Proprietary Information. This Agreement does not require, nor may it be implied that any Party shall be required to disclose any particular Proprietary Information to any other Party hereunder. For purposes of this Agreement, "Proprietary Information" shall mean all technical, business, financial and other information related to the Subject which is furnished by one Party ("Originating Party") to another Party ("Receiving Party"):

   (i)   in written or other tangible form marked with a proprietary legend, or

   (ii)   in electronic form where any display of the information also displays a proprietary legend, or such legend is marked on the media containing such information; or

   (iii)   via any computer or terminal to which the Receiving Party is permitted access at an Originating Party's facility or which, regardless of location, requires entry by the Receiving Party of a password or key prior to access being permitted, whether or not such information is separately marked or identified as Originating Party Proprietary Information; or

   (iv)   in oral or visual form, identified as being proprietary at the time of disclosure and thereafter summarized in a writing that identifies the information as being proprietary and is transmitted to the Receiving Party within (30) days after the oral or visual disclosure. During the thirty (30) day period, the information so disclosed and identified shall be protected and handled as Proprietary Information in accordance with the provisions of this Agreement.

In the event that a Originating Party inadvertently or accidentally fails to identify information furnished to the other Party as being Proprietary Information in accordance with the forgoing, the Originating Party may correct such inadvertence or accident by notifying the Receiving Party in writing promptly after the discovery thereof; provided, however, that the Receiving Party shall have no liability whatsoever with respect to any disclosures or uses of the unidentified or unmarked Proprietary Information which may have occurred prior to receipt of such written notification. An Originating Party will not identify information as Proprietary Information unless they believe that such information is proprietary or constitutes a trade secret. The Originating Party will attempt to limit the exchange of Proprietary Information, disclosing to the Receiving Party only that Proprietary Information which the Originating Party believes necessary for the Purpose of this Agreement.

2)   Period of Protection.   The "Period of Protection" during which Proprietary Information received pursuant to this Agreement shall be subject to an obligation of confidentiality and protection, and subject to restrictions on handling, disclosure and use, shall extend until three (3) years after the date of termination of this Agreement.

3)   Standard of Care.   A Receiving Party shall take such steps as are reasonably necessary to preserve in confidence all Proprietary Information disclosed to it pursuant to this Agreement, but not less than the care which the Receiving Party normally employs to protect and safeguard the confidentiality of its own proprietary information of like kind which it does not wish disseminated or misused. Any third party Proprietary Information to which the Receiving Party is afforded access pursuant to this Agreement shall be protected and handled by the Receiving Party in the same manner as required herein for Proprietary Information belonging to the Parties hereto. Neither Party shall provide access to third party Proprietary Information unless it has the third party's authorization to do so.

4)   Protection and Handling of Proprietary Information.   THE PARTICIPATING PARTIES and LOCKHEED MARTIN agree that, unless it has the prior written permission of the other Party:

(i)   it will not disclose any of the Proprietary Information received hereunder to any third party;

(ii)   it will copy only such portions of the Proprietary Information received hereunder as may reasonably be necessary to carry out the above stated Purpose, provided that each such copy, whether in whole or in part, includes a reproduction of all proprietary markings and legends contained on the original which pertain to the copied portions;

(iii)   it will permit access to Proprietary Information received hereunder only by those of its officers and employees who have a need-to-know in order to carry out the above stated Purpose, provided that each such person is informed by the Receiving Party that the information is Proprietary Information belonging to the Originating Party and as such, is subject to protection and handling in accordance with the terms of this Agreement and

(iv)   except as defined in the Lockheed Martin SOW, it will not attempt to determine the content or structure, or otherwise reverse engineer any material sample, hardware or software to which it is provided access pursuant to this Agreement.

5)   Permissible Disclosures.   In order to carry out the intended Purpose of this Agreement for the mutual benefit of both Parties hereto, each Party may disclose Proprietary Information received hereunder:

(i)   to any third party that is participating with the Parties hereto in the Subject of this Agreement, to the extent such disclosure is necessary for the third party to

interface with the Parties hereto or their respective products in carrying out the above stated Purpose; provided, that, such third party has entered into a written agreement of confidentiality with the Originating Party, and that the Receiving Party notifies the Originating Party in writing prior to any such disclosure and follows any specific limitations or restrictions imposed on the disclosure by the Originating Party; and

(ii)   to contract labor personnel used in the Receiving Party's business operations who have a need-to-know the Proprietary Information for the Purpose of this Agreement, provided, that, such personnel are under a written obligation to hold the Proprietary Information in confidence under terms and conditions at least as restrictive as the terms and conditions of this Agreement; and

(iii)   to any publication after obtaining the express written consent of Ken Sargent or Susan Lewis as described in the above stated Purpose.

6)   <u>Restriction on Use.</u> The Receiving Party may use the Proprietary Information received hereunder solely for the aforementioned Purpose. No other use is permitted without the prior written permission of the Originating Party. Without limiting the foregoing, a Receiving Party shall not use any of the Originating Party's Proprietary Information to design, develop, modify or fabricate any product without the prior express written permission of the Originating Party, and then only to the extent that such use complies fully and specifically with all conditions imposed by the Originating Party in such express written permission.

7)   <u>Exceptions to Duty</u>. This Agreement does not restrict disclosure or use of information otherwise qualifying as Proprietary Information if the Receiving Party can show by documented evidence that any one of the following conditions exists:

(i)   the information was already in the public domain when the Originating Party disclosed it to the Receiving Party, or entered the public domain after the Originating Party disclosed it under this Agreement, but through no fault of the Receiving Party;

(ii)   the Receiving Party knew the information and held it without restriction as to further disclosure and use when the Originating Party disclosed the information under this Agreement;

(iii)   another source lawfully disclosed the information to the Receiving Party and did not restrict the Receiving Party in its further disclosure or use;

(iv)   the Receiving Party developed the information independently, by personnel who did not have access to the Originating Party's information;

(v)   the Period of Protection has expired;

(vi) the information was disclosed in response to a subpoena or court order duly issued in a judicial or legislative process, provided that the subpoenaed Party notified the Originating Party of the subpoena at least five days prior to the disclosure, unless such notice could not reasonably be given, and the subpoenaed Party cooperated with the Originating Party in appealing the disclosure or obtaining a protective order.

8) <u>Inadvertent Disclosure or Use</u>. The Receiving Party shall not be liable for accidental or inadvertent disclosure or use of Proprietary Information received pursuant to this Agreement, if such Receiving Party shows that the above Standard of Care was employed in the protection and handling of the Originating Party's Proprietary Information, and that upon discovery, the Receiving Party made a reasonable effort to retrieve any such accidentally or inadvertently disclosed Proprietary Information, ceased all unauthorized use, and took such additional measures as may reasonably have been required under the circumstances to prevent any further unauthorized disclosure and use of the Originating Party's Proprietary Information.

9) <u>Ownership of Proprietary Information</u>. Each Party represents that it owns or otherwise has the right to furnish to the other Party all information transferred to the other Party hereunder.

10) <u>Restrictions on Export</u>. Neither Party shall disclose any Proprietary Information or other information furnished hereunder in any manner contrary to the laws and regulations of the United States of America. Both parties agree that it will not transfer any export controlled item, data, or service, to include transfer to foreign persons, as defined in ITAR 22 CFR 120.16, employed by or associated with, or under contract to either Party or either Party's lower-tier suppliers (including but not limited to any professors or students who are foreign persons, as defined in ITAR 22 CFR 120.16), without the authority of an export license, agreement, or applicable exemption or exception. Each party shall indemnify and hold harmless the other for any fines or other damages resulting from violations of any such laws and regulations.

11) <u>No Warranty or Liability</u>. NEITHER PARTY MAKES ANY WARRANTY, EXPRESS OR IMPLIED, WITH RESPECT TO INFORMATION FURNISHED TO THE OTHER HEREUNDER INCLUDING, WITHOUT LIMITATION, NO EXPRESS OR IMPLIED WARRANTIES OF MERCHANTABILITY, FITNESS FOR A PARTICULAR PURPOSE, FREEDOM FROM DEFECTS, FREEDOM FROM TRADE SECRET, PATENT OR COPYRIGHT INFRINGEMENT, ADEQUACY, ACCURACY OR SUFFICIENCY, WHETHER ARISING BY LAW, CUSTOM OR CONDUCT. AN ORIGINATING PARTY SHALL NOT BE LIABLE TO A RECEIVING PARTY FOR ANY DAMAGES THAT MAY RESULT FROM THE RECEIVING PARTY'S RECEIPT OR USE OF, OR RELIANCE ON INFORMATION FURNISHED HEREUNDER, REGARDLESS OF WHETHER THE ORIGINATING PARTY WAS AWARE OF THE POSSIBILITY OF SUCH

DAMAGES OR NOT, NOR SHALL EITHER PARTY BE LIABLE TO THE OTHER FOR ANY INCIDENTAL, SPECIAL, CONSEQUENTIAL, PUNITIVE OR MULTIPLE DAMAGES.

12) Independent Contractors. The Parties hereto are and shall remain independent contractors. This Agreement shall not constitute, create, give effect to, or otherwise imply an employment relationship, teaming arrangement, joint venture, pooling arrangement, partnership, or formal business organization of any kind, nor does this Agreement or the disclosure or receipt of any information hereunder constitute an offer, acceptance, promise or obligation by either Party to enter into any contract, subcontract, amendment, agreement or other business relationship with the other Party. Unless otherwise agreed in writing, each Party shall perform hereunder solely at its own cost and expense.

13) No License. Nothing in this Agreement shall be deemed to grant a license, directly or by implication, estoppel, or otherwise, under any intellectual, industrial, or other property right associated with any information disclosed under this Agreement, whether such information is Proprietary Information or not. Without limiting the foregoing, no right in, or license under, any present or future proprietary information, trade secret, invention, patent, copyright, mask work, trade name or trademark is either offered or granted under this Agreement.

14) No Purchase Obligation. No Party has an obligation under this Agreement to purchase any product or service from any other Party, to offer for sale any product using or incorporating the Proprietary Information of any other Party, to enter into a business relationship with any other Party, or to refrain from engaging in a relationship with any individual Party independently of any other Party or with any third party. Further, no Party has an obligation to provide Proprietary Information to any other Party as the result of entering into this Agreement. Nothing in this Agreement shall be construed as a representation that any Party will not pursue similar opportunities independently, or with any third parties, provided that the obligations of this Agreement are not breached.

15) Assignment. Neither LOCKHEED MARTIN nor THE PARTICIPATING PARTIES shall assign, nor in any manner transfer, any information received hereunder or its interests in this Agreement or any part hereof, without first obtaining the prior written approval of the other Parties. Such approval shall not be unreasonably withheld where the assignment is being made to a successor corporation in the event of a corporate name change or merger, or to a purchaser of that portion of the assignor's business to which the subject of this Agreement pertains.

16) Withdrawal by a Party. Any Party may withdraw from this Agreement by giving thirty (30) days notice in writing to the remaining Parties. Withdrawal shall not, however, relieve the withdrawing Party of any of its obligations contained herein with respect to information received by the Party prior to withdrawal.

17) <u>Term and Termination.</u> This AGREEMENT shall (unless extended by written mutual agreement) automatically terminate on 1 June 2015, but may be terminated earlier by mutual agreement of the Parties. Termination shall not, however, affect the rights and obligations contained herein with respect to Proprietary Information received prior to termination; such rights and obligations with respect to such Proprietary Information shall survive termination of this Agreement until the Period of Protection set forth above has expired.

18) <u>Return or Destroy.</u> A Receiving Party will, upon written request from the Originating Party, use reasonable efforts to destroy all copies of the Proprietary Information received from the Originating Party hereunder, including any copies made by the Receiving Party, and certify their destruction to the Originating Party. Alternately, if the Originating Party so requests, the Receiving Party shall return all such copies to the Originating Party. Notwithstanding the foregoing, a Receiving Party may retain a single archival copy of the received Proprietary Information which may be used solely for legal evidentiary purposes in the event of a dispute arising under this Agreement.

19) <u>Controlling Law.</u> This Agreement shall be governed by and interpreted in accordance with the laws of the State of Florida, United States of America, but without reference to its conflict of law provisions.

20) <u>Notices.</u> Any notices and Proprietary Information not furnished in person shall be transmitted either electronically or by mail to Lockheed Martin at:

LOCKHEED MARTIN CORPORATION
5600 Sand Lake Road   Mail Stop MP-274
Orlando, Florida 32819 U.S.A.
Attention: Susan Lewis

and to Kevin Coffy at:

KEVIN COFFY
5600 Sand Lake Road   Mail Stop kcoffy@knights.ucf.edu
Orlando, Florida 32819 U.S.A.
Attention: 561-866-1404
Email: kcoffy@knights.ucf.edu
Phone: 5618661404

and to University Of Central Florida at:

UNIVERSITY OF CENTRAL FLORIDA
Office of Research & Commercialization
12201 Research Parkway, Suite 501
Orlando, Florida 32826 U.S.A.
Attention: Andrea Adkins
Email: Andrea.Adkins@ ucf.edu

Any Party may change its respective address or representative at any time by written notice given to the other Parties.

21)   Entirety. This Agreement contains the entire understanding between the Parties relative to the protection, handling and use of Subject Proprietary Information, and supersedes all prior and collateral communications, reports, and understandings between the Parties in respect thereto. No change, modification, alteration, or addition to any provision hereof shall be binding unless in writing and signed by authorized representatives of both Parties. Invalidity or unenforceability of any provision of this Agreement shall not limit or impair the operation or validity or enforceability of any other provision hereof.

22)   Counterparts. This Agreement may be executed in counterparts, all of which shall be considered one and the same Agreement, and shall become effective when all of the counterparts have been signed by the Parties to this Agreement and delivered to each of the other parties. Copies shall be considered as originals.

AS EVIDENCE OF MUTUAL AGREEMENT to the foregoing terms and conditions by the Parties hereto, the Parties have executed this PROPRIETARY INFORMATION AGREEMENT on the date(s) shown herein below. The "Effective Date" shall be the date of signature by the last executing Party.

LOCKHEED MARTIN CORPORATION

[signature]

Authorized Signature

MECHANICAL ENG. MGR,
Title

6-19-2013
Date

KEVIN COFFY

[signature]

Authorized Signature

UCF Student and LM CWEP Participant
Title

06/17/2013
Date

UNIVERSITY OF CENTRAL FLORIDA
by and on behalf of its Board of
Trustees

[signature]

Authorized Signature

Andrea Adkins

Title

Assistant Director, Technology Transfer

Date

REFERENCES

AK Steel Corporation. (2007, Jan 8). *15-5_ph_data_sheet.* Retrieved from www.aksteel.com:

    http://www.aksteel.com/pdf/markets_products/stainless/precipitation/15-

    5_ph_data_sheet.pdf

ASHOK KUMAR, Y. B. (2013). Indigenous Development and Airworthiness Certification of

    15–5 PH Precipitation Hardenable Stainless Steel for Aircraft Applications. In

    Sadhana (Vol. Vol. 38 Part 1, pp. 3-23). Indian Academy of Sciences.

ASM International. (1992). Volume 9 - Metallography and Microstructures. In A. I.

    Commitee, *ASM Metals Handbook.* Materials Park, Ohio, USA: ASM International.

ASM International. (2005). Volume 1 Properties and Selection of Iron. In A. I. Committee,

    ASM Handbook (pp. 1350-1352). Materials Park, OH: ASM International.

ASTM International. (2007). E407-07 Standard Practice for Microetching Metals and Alloys.

    West Conshohocken, PA, USA.

ASTM International. (2011). ASTM E1019-11 Standard Test Methods for Determination of

    Carbon, Sulfur, Nitrogen and Oxygen in Steel, Iron, Nickel and Cobalt Alloys by

    Various Combustion and Fusion Techniques . West Conshohocken, PA, USA.

ASTM International. (2013). A564/A564M-13 Standard Specification for Hot-Rolled and

    Cold-Finished Age-Hardening Stainless Steel Bars and Shapes. West Conshohocken,

    PA, USA.

ASTM International. (2013). ASTM E112-13 Standard Methods for Determining Average

    Grain Size. West Conshohocken, PA, USA.

ASTM International. (2013). E975-13 Standard Practice for X-Ray Determination of

    Retained Austenite in Steel with Near Random Crystallographic Orientation. West

    Conshohocken, PA, USA.

Aulus Roberto Romão Bineli, A. P. (2011). Direct Metal Laser Sintering (DMLS): Technology

    for Design and Construction of Microreactors. *6th Brazilian Conference on*

    Manufacturing Engineering (pp. 1-7). Caxias do Sul: ABCM.

Bajguirani, H. H. (2002). The Effect of Ageing Upon the Microstructure and Mechanical

    Properties of Type 15-5PH Stainless Steel. *Materials Science and Engineering A*, 142-

    159.

C. J. Long, W. T. (1973). The Ferrite Content of Austenitic Stainless Steel Weld Metal.

    American Welding Society Annual Meeting (pp. 281-S to 179-S). Chicago: Welding

    Journal.

Cdang - Original Work, T. -D. (2009, October 2). *File:Cast ingot macrostructure.svg*.

    Retrieved from Wikimedia Commons:

    http://commons.wikimedia.org/wiki/File:Cast_ingot_macrostructure.svg

Cdang. (2009, May 29). *File:Diagramme schaeffler.svg.* Retrieved from Wikimedia

    Commons: http://commons.wikimedia.org/wiki/File:Diagramme_schaeffler.svg

Cullity, B. D. (1956). *Elements of X-Ray Diffraction.* Reading, MA: Addison-Wesley Publishing

    Company, Inc.

EOS GmbH - Electro Optical Systems. (2012, October 23). *EOS-StainlessSteel-PH1.* Retrieved

    from http://www.eos.info/: http://www.eos.info/material-m

Joel I. Gersten, F. W. (2001). *The Physics and Chemistry of Materials.* New York: John Wiley &

    Sons, Inc.

Materialgeeza. (2008, May 11). Selective laser melting system schematic. By Materialgeeza

    (Own work) [CC-BY-SA-3.0 (http://creativecommons.org/licenses/by-sa/3.0) or

    GFDL (http://www.gnu.org/copyleft/fdl.html)], via Wikimedia Commons. Retrieved

    from

http://commons.wikimedia.org/wiki/File:Selective_laser_melting_system_schemati
c.jpg

Materials Data Incorporated. (2011). JADE Software. Livermore, California.

P.P. Bandyopadhyay, D. C. (2013). Influence of Sinking-in and Piling-up on the Mechanical
Properties Determination by Indentation: A Case Study on Rolled and DMLS
Stainless Steel. *Materials Science & Enineering A*, 126-133.

Pace Technologies. (2013). *Safety Data Sheet Vilella's Reagent.* Retrieved from
www.metalographic.com:
http://www.metallographic.com/MSDS/Vilellas%20Reagent.pdf

R. E. Smallman, A. H. (2007). *Physical Metallurgy and Advanced Materials, Seventh Edition.*
Burlington, MA: Butterworth-Heinemann.

Rober W. Balluffi, S. M. (2005). *Kinetics of Materials.* Online: John Wiley & Sons, Inc.

SAE International. (2008, Sept). AMS2759/3E. Warrendale, PA, USA.

Schaeffler, A. L. (1949). Constitution diagram for stainless steel weld metal. *Metal Progress
Vol. 56*, pp. 680 - 680B.